Golgin45 SUMOylation Contributes To PML Nuclear Body Formation During Heat Shock Response

Shuaiyang Jing
ShanghaiTech University
Jingkai Gao
ShanghaiTech University
Neeraj Tiwari
Yale University
Yulei Du
ShanghaiTech University
Lianhui Zhu
ShanghaiTech University
Bopil Gim
ShanghaiTech University
Yi Qian
ShanghaiTech University
Xihua Yue
ShanghaiTech University
Intaek Lee (Leeintaek@shanghaitech.edu.cn)
ShanghaiTech University https://orcid.org/0000-0003-1084-674X

Research Article

Keywords: Golgin45, SUMO, PML, PML nuclear bodies, heat shock, Golgi apparatus, PARylation, Tankyrase, Importin-β2

Posted Date: April 5th, 2022

DOI: https://doi.org/10.21203/rs.3.rs-1485254/v1

Golgin45 SUMOylation Contributes To PML Nuclear Body Formation During Heat Shock Response

Shuaiyang Jing[1,4]*, Jingkai Gao[1,4]*, Neeraj Tiwari[2], Yulei Du[1,4], Lianhui Zhu[1], Bopil Gim[3], Yi Qian[1]†, Xihua Yue[1]† and **Intaek Lee**[1]†

[1] School of Life Science and Technology, ShanghaiTech University, Shanghai, China

[2] Department of Cell Biology, Yale University School of Medicine, New Haven, CT 06520 USA

[3] School of Physical Science and Technology, ShanghaiTech University, Shanghai, China

[4] University of Chinese Academy of Sciences, Beijing, China

*These authors contributed equally to this work.

†To whom correspondence may be addressed. Email: yuexh@shanghaitech.edu.cn ; qianyi@shanghaitech.edu.cn ; Leeintaek@ShanghaiTech.edu.cn

Keywords: Golgin45, SUMO, PML, PML nuclear bodies, heat shock, Golgi apparatus, PARylation, Tankyrase, Importin-β2

Abstract

SUMOylation is a post-translational modification that attaches a ubiquitin-like modifier to target proteins and plays a number of roles throughout the cells, including transcriptional regulation and cellular stress response, etc. We have recently reported that a Golgi structural protein, Golgin45, is subjected to Tankyrase1-dependent poly (ADP-Ribosyl)ation, resulting in dynamic regulation of Golgin45 protein and membrane trafficking of glycosylating enzymes at the Golgi. However, exact mechanism that modulates Tankyrase activity on Golgin45 remained elusive. Here, we report that Golgin45 is a SUMOylated protein, and heat shock significantly increases Golgin45 SUMOylation, concomitantly leading to reduced PARylation. Importantly, while PML is required for Golgin45 SUMOylation by SUMO3, over-expression of a SUMOylation-deficient Golgin45 mutant inhibits the formation of PML-NBs under heat shock, revealing a role of SUMOylated Golgin45 in PML-NB formation in the nucleus. These results provide a new insight into stress-induced inter-organelle communications between the Golgi and the nucleus.

Introduction

Small ubiquitin-like modifier (SUMO) is a well-known post-translational modification that is covalently attached to lysine residues of hundreds of target proteins (*1*). Unlike ubiquitination, SUMO modification likely occurs at SUMO consensus sequence, ΨKxE (Ψ= hydrophobic residue, x = any amino acid residue), although it is also known to be attached to non-consensus sites under stress condition (*2-4*).

In mammals, five SUMO isoforms have been identified to date (*5*). A number of studies have shown that these SUMO isoforms play different roles in various physiological contexts, and there is also high functional redundancy, which had made it difficult to study their specific functions (*1, 5, 6*). While the most extensively studied SUMO isoform is SUMO1, SUMO1 is largely dispensable for mouse embryonic development, whereas SUMO2/3 play more crucial roles (*7*). SUMOylation has been shown to modulate protein-protein interaction, intracellular localization of proteins, enzymatic activity, immune cell functions, cellular stress response and inflammatory responses, etc (*6*).

One of the well characterized roles for protein SUMOylation is regulation of promyelocytic leukemia nuclear bodies (PML-NBs) formation, which undergoes dynamic regulation by protein SUMOylation (*8-10*). PML-NBs are involved in various genome maintenance pathway and cellular stress response, including the DNA damage response, innate immunity during viral infection, DNA repair, telomere homeostasis, cellular senescence and p53-associated apoptosis (*11-14*).

We have recently reported that Golgin45, a Golgi structural protein, functions as a major docking factor for Tankyrase-1 (TNKS1) recruitment to Golgi membranes, and that TNKS1-dependent poly (ADP-ribosyl)ation (PARylation) of Golgin45 regulates Golgin45 protein level via proteasomal degradation in interphase cells, leading to modulation of intracellular trafficking dynamics of Golgi-resident glycosyltransferases (*15*). These results revealed a novel regulatory mechanism that influences Golgi structure and function via PARylation of its structural protein. Yet, exactly how TNKS1-dependent Golgin45 PARylation is controlled had remained elusive.

A number of studies have suggested that ubiquitination, PARylation and SUMOylation influence one another in various physiological and pathological conditions (reviewed in (*16*)). In order to further investigate the regulatory mechanism behind TNKS1-dependent Golgin45 PARylation, we posited that

Golgin45 may be subjected to both PARylation and SUMOylation and the interplay between them might modulate the steady state level of Golgin45 protein during interphase.

Our new results show that Golgin45 is a heavily SUMOylated protein with at least 8 SUMOylation sites primarily in its N-terminal domain and its SUMOylation is facilitated by Importin-β2-mediated translocation into the nucleus. Importantly, Golgin45 SUMOylation is greatly increased up on cellular stress, such as heat shock stress. Whereas Golgin45 is mostly modified by SUMO1 under steady state condition, SUMO2/3 conjugation was specifically increased under heat shock stress, facilitating its inclusion into PML-NBs. In support of these results, PML depletion inhibited SUMO3 conjugation to Golgin45, and expression of SUMOylation deficient Golgin45 mutants significantly inhibited the formation of PML-NBs, suggesting that SUMOylated Golgin45 may assist in efficient PML-NB formation during heat shock response.

Taken together, these results strongly suggest that SUMOylated Golgin45 may provide an inter-organelle communication between the Golgi and the nucleus for modulation of cellular stress response by influencing PML-NB formation.

Results

Golgin45 is a SUMOylated protein

In order to test whether Golgin45 can be modified by SUMO, we initially used TAK981 (SUMO E1 inhibitor) and checked whether it influences protein level of endogenous Golgin45. To this end, HeLa cells were treated with either 5 μM XAV939 (that stabilizes Golgin45 protein by inhibiting its PARylation (*15*)) or 10 μM TAK981 for various time points up to 24 hours. Cells were then lysed in RIPA buffer and subjected to western analysis using anti-Golgin45, GRASP55, ACBD3, Tankyase1/2 and GAPDH, respectively. The results showed that TAK981 significantly reduced Golgin45 protein level, whereas XAV939 greatly stabilized endogenous Golgin45 protein during the tested time frame (**Figure 1A**).

To confirm this finding, we repeated this experiment by treating the cells using increasing concentrations of TAK981 for 24 hours, as indicated in the **Figure 1B**. The results indicated that

increasing TAK981 concentration had progressively more destabilizing effect on endogenous Golgin45 protein, as expected. Taken together, these results showed that Golgin45 protein is likely to be regulated by SUMOylation.

Next, HeLa cells were transiently transfected with mCherry-Golgin45, FLAG-Ubc9 WT (a SUMO E2 conjugase) or dominant negative mutant (DN) and myc-SUMO1 overnight, followed by treatment with or without TAK981 for 12 hours, in order to directly test Golgin45 conjugation to SUMO1. Cells were then lysed in RIPA buffer and subjected to western blots for changes in Golgin45 protein.

The results showed multiple bands of mCherry-Golgin45 above the typical ~75 kDa band, indicating that Golgin45 is likely to be SUMOylated at multiple sites (**Figure 1C;** compare lane 1 and 2). In addition, the observed upper bands of Golgin45 were greatly reduced by treatment with TAK981 (**Figure 1C**; compare lane 2 and 4), confirming the finding that Golgin45 is indeed a SUMOylated protein.

To explore how Golgin45 SUMOylation may be regulated, cells were similarly transfected with mCherry-Golgin45, FLAG-Ubc9 WT (or dominant negative) and myc-SUMO1 overnight, followed by glucose starvation, Torin1 (inducer of autophagy), DOXO (DNA damage), TAK243 (ubiquitin E1 inhibitor), TAK981 and tert-Butylhydroquinone (TBHQ; oxidative stress) for 12 hours (**supplementary Figure 1A**). Other than Torin1 and TAK981 treatment, both of which reduced SUMOylation, we didn't notice any other significant change in Golgin45 SUMOylation, suggesting that Golgin45 SUMOylation by SUMO1 may also be modestly influenced by autophagy, which requires future study.

In order to investigate whether Golgin45 SUMOylation is restricted to SUMO1 only, we transfected HeLa cells with either Ubc9 WT or DN along with mCherry-Golgin45 and myc-SUMO1 or myc-SUMO2/3, followed by western analysis. As expected, Ubc9 DN failed to induce higher molecular weight SUMOylated Golgin45 bands (**Figure 1D**; compare lane 1 and 2). Interestingly, we detected evidence of Golgin45 SUMOylation by SUMO2/3 as well as SUMO1, although SUMO2/3 modification was much weaker than SUMO1 under steady state condition (**Figure 1D**; compare lane 2 and 4).

We then decided to search for potential SUMOylation sites on Golgin45 protein. Since C-terminal deletion may cause significant disruption of Golgin45 targeting to the Golgi (*17*), we initially compared N-terminal deletion mutant of Golgin45 (121-400) with the full length mCherry-Golgin45. HeLa cells

were transfected with these two Golgin45 constructs along with FLAG-Ubc9 WT (or DN) and myc-SUMO1. Strikingly, Golgin45 (121-400) failed to show the typical SUMOylated Golgin45 upper bands (**Figure 1E**; compare lane 1 and 2), suggesting that the majority of SUMOylation sites likely occur in the N-terminal one third of Golgin45 protein. These results allowed us to significantly narrow down the potential lysine residues to mutate in a mutagenesis study to identify the SUMOylation sites on Golgin45.

Next, each lysine (K) residues in the N-terminal region of Golgin45 were mutated to arginine (R) and we performed a mutagenesis study using mCherry-Golgin45, Flag-Ubc9 and myc-SUMO1 to search for SUMOylation sites on Golgin45. The results showed that mutation of lysine residues at positions 4, 9, 67, 72, 77, 100, 106, 127 largely eliminated the multiple SUMOylated bands (**Figure 1F-G**; compare lane 2 and 9). This eight-lysine mutant (8-KR) also failed to show the multiple SUMOylated bands, when the cells were transfected with either myc-SUMO2 or myc-SUMO3, indicating that SUMO1 and SUMO2/3 likely share similar SUMOylation sites for Golgin45 to a significant extent (**Figure 1H**).

Since as many as eight lysine residues were changed into Arginine, we were concerned that these mutations may have unforeseen and unexpected effect on Golgin45 protein. In an effort to more thoroughly study post-translational modifications of Golgin45 that influence its protein stability, we also managed to locate the three lysine residues for ubiquitination in the C-terminal region of Golgin45, as illustrated in the schematic of Golgin45 (**Figure 1G)**. Mutation of these three lysine residues to arginine (K350/370/371R) greatly enhanced protein stability of Golgin45 to an extent of TNKS1-binding domain deletion mutant of Golgin45 (ΔTBD) (**supplementary Figure 2**). In addition, estimation of protein half-life using a cycloheximide (CHX) protocol indicated a similar increase in protein stability for K350/370/371R mutant and ΔTBD mutant of Golgin45 (**supplementary Figure 2**; see the graph in the lower panel).

To test whether Golgin45 SUMOylation is monomeric or multimeric in its nature, HeLa cells were transfected with either myc-SUMO1 K7/16/17R or myc-SUMO3-K11R that block multimer formation of these SUMO isoforms (*1, 7, 18*) along with Flag-Ubc9 and mCherry-Golgin45 overnight, followed by western analysis. The results showed that expression of myc-SUMO1-K7/16/17R had no significant effect on Golgin45 SUMOylation, compared to the control myc-SUMO1, whereas my-SUMO3-K11R greatly reduced SUMO3 conjugation to Golgin45 (**Figure 1I-J**). These results suggested that SUMO1 modification on Golgin45 is likely to be monomeric, while SUMO3 modification is likely to be multimeric and/or branched in its nature.

SUMOylation enhances Golgin45 protein stability by inhibiting TNKS1-dependent PARylation of Golgin45

We have recently shown that Golgin45 protein stability is under strict regulation by TNKS1-dependent PARylation and subsequent proteasomal degradation (*15*). In order to study whether there exists an interplay between SUMOylation and PARylation of Golgin45, HeLa cells were transiently transfected with mCherry-Golgin45 and SUMO1 along with Ubc9 WT or DN, followed by treatment with either DMSO or XAV939 (a specific inhibitor of TNKS1/2) (*15*).

The results showed that XAV939 treatment greatly increased SUMOylation on Golgin45 (**Figure 2A**; compare SUMOylated upper bands in lane 2 and 4), although XAV939 treatment also increased overall Golgin45 protein stability. Deletion of TNKS1 binding domain (ΔTBD) showed a similar increase in Golgin45 SUMOylation as XAV939 treatment (**Figure 2B**; lane 2 and 4). Taken together, these results suggested that inhibition of TNKS1 activity likely enhances Golgin45 SUMOylation. Similar increase in SUMO3 conjugation was also observed in Golgin45 ΔTBD mutant (**Figure 2C**).

Since increased SUMOylation of Golgin45 in XAV939-treated cells and Golgin45 ΔTBD mutant appeared to coincide with overall enhancement of Golgin45 protein stability, we attempted to measure the changes in its protein half-life that can be more directly attributed to SUMOylation only. To this end, HeLa cells were transfected with mCherry-Golgin45 WT or Golgin45 (8-KR) mutant, followed by the CHX protocol as described previously in the methods. The results indicated that Golgin45 (8-KR) mutant, a SUMO-deficient mutant, showed significantly decreased protein half-life, as shown in **Figure 2D**, compared to the WT control, demonstrating that SUMOylation indeed enhances Golgin45 protein stability on its own.

Furthermore, we found using anti-PAR western blots that mCherry-Golgin45 is strongly PARylated, which can be inhibited by increased SUMOylation via co-transfection of Flag-Ubc9 and myc-SUMO1 (**Figure 2E**; compare lane 2 and 3). We also observed that PARylation is greatly increased for Golgin45 8-KR mutant, compared to the WT control (**Figure 2F**; compare lane 2 and 3). Taken together, these results indicated that SUMOylation and PARylation of Golgin45 are likely to be in a dynamic interplay under steady state condition, providing a regulatory mechanism for Golgin45 protein stability.

Inhibition of Golgin45-Importinβ2 binding abrogates Golgin45 SUMOylation

It is well known that SUMOylation plays crucial roles in the nucleus, such as PML-NB formation under cellular stress (*1, 13*). Golgin45 was originally identified as a nuclear co-factor, JEM-1, that is up-regulated during retinoid-induced maturation of NB4 promyelocytic leukaemia, prior to its characterization as a Golgi structural protein, Golgin45 (*17, 19*). We reasoned that SUMOylation of Golgin45 might be relevant to its localization and/or function in the nucleus, as opposed to TNKS1-mediated PARylation of Golgin45 providing its regulatory mechanism at the Golgi (*15*).

Thus, we decided to look for the nuclear localization signal (NLS) of Golgin45, in order to better understand its SUMOylation mechanism and nuclear import. A careful search for NLS led to identification of a non-classical PY NLS (^{375}**RxxPY**^{379}) in the C-terminal region of Golgin45 (*20*), as illustrated in **Figure 3A**. We then expressed and purified a Golgin45 fragment (amino acids 336-385) fused to GST from bacteria and performed GST-pulldown assays with GST-Golgin45 (336-385) WT or the R375A mutant and purified Importin β2. The results showed that R375A mutation completely abrogates Golgin45 binding to Importin β2 (**Figure 3B**; compare lane 3 and 4). Immunoprecipitation experiments confirmed this finding, although there was still some residual binding between R375A mutant and Importin β2 (**Figure 3C**; compare lane 5 and 6).

To verify this finding further using confocal microscopy, HeLa cells were transfected with either mCherry-Golgin45 or mCherry-Golgin R375A mutant overnight, followed by indirect staining with anti-GM130 (a Golgi marker) antibody and DAPI (nuclear staining). The results showed that mCherry-Golgin45 WT showed intense fluorescence both at the Golgi and in the nucleus, whereas Golgin45 R375A mutant showed strong fluorescence at the Golgi, but failed to localize to the nucleus, as expected (**Figure 3D-E**).

Strikingly, R375A mutation almost eliminated SUMO1 conjugation to Golgin45, as shown in **Figure 3F**, suggesting that Importin β2-mediated nuclear targeting is required for efficient Golgin45 SUMOylation by SUMO1. On the other hand, V214/273A mutant (which blocks its binding to Rab2-GTP) or S15D (CDK1 phosphorylation mimicking mutant) Golgin45 showed slight reduction in Golgin45 SUMOylation. Similarly, SUMO3 conjugation to Golgin45 was also reduced for R375A mutant (**Figure 3G**). These results

demonstrate that Importin-β2-mediated nuclear import of Golgin45 plays an important role in Golgin45 SUMOylation.

Heat shock stress greatly increases Golgin45 conjugation to SUMO2/3 in the nucleus

In order to test the possibility that SUMOylation itself may also positively reinforce Golgin45 import and retention in the nucleus, HeLa cells were transfected with mCherry-Golgin45, myc-SUMO1 (or SUMO3) and FLAG-Ubc9 WT or DN overnight. Cells were then lysed in TX-100-based lysis buffer, and post-nuclear fraction was separated from cytosolic fraction using low speed 1,000xg centrifugation protocol. The samples were then mixed with SDS-sample buffer and analyzed by western blots. The results showed that Golgin45 was relatively more enriched in the nuclear fraction for cells transfected with SUMO1 (**Figure 4A**; compare lane 5 and 6).

Strikingly, SUMOylated Golgin45 was almost exclusively found in the nuclear fraction in cells transfected with SUMO3 (**Figure 4B**; compare upper bands in lane 5 and 6), suggesting that SUMO3 modification may further enhance nuclear retention of Golgin45, compared to SUMO1 modification. This finding is consistent with previous reports that SUMO1 and SUMO3 modification play functionally distinct roles for SUMOylated proteins (*21, 22*).

As SUMOylation has been associated with stress response pathways (*23*), we then posited that cellular stress may play a role in Golgin45 targeting to the nucleus. In particular, we asked whether heat shock stress may be linked to Golgin45 import into the nucleus, especially since Golgin45 protein level significantly influences protein secretion and maturation at the Golgi, which had been known to be profoundly influenced by temperature (*15, 24, 25*).

To study whether heat shock stress may influence nuclear import of Golgin45, HeLa cells were transfected with either control mCherry or mCherry-Golgin45 overnight, followed by heat shock at 43 °C (or control 37 °C) for 1 hour. The cells were then lysed and subjected to the same low speed centrifugation protocol to separate the nucleus from the post-nuclear supernatant, followed by western analysis.

The results showed that cytosolic fraction of mCherry-Golgin45 was greatly reduced after 1 hour of heat shock treatment (**Figure 4C**; compare lane 6 and 12), whereas there was no obvious change in control mCherry protein. Consistent with this reduction in the cytosolic fraction, there was a corresponding increase in nuclear fraction of mCherry-Golgin45 (**Figure 4C**; compare lane 5 and 11), indicating increased nuclear import of Golgin45 under heat shock stress. Overall, these results suggested that nuclear localization of Golgin45 likely increases under heat shock stress.

Next, we checked whether heat shock stress influences the stability of Golgin45 protein by western blots against endogenous Golgin45. To this end, HeLa cells were subjected to heat shock stress for 0, 2, 4 and 6 hours, followed by cell lysis in SDS sample buffer and western analysis using indicated antibodies (**Figure 4D**). The results showed that endogenous Golgin45 protein level increased significantly up on heat shock stress (**Figure 4D**). As controls, we also blotted for endogenous GM130 and known binding partners of Golgin45, including ACBD3, GRASP55 and TNKS1 as well as β-actin (loading control), all of which showed no significant changes after heat shock treatment. These results suggested that heat shock stress may significantly influence Golgin45 import into the nucleus and protein stability of Golgin45, by altering Golgin45 SUMOylation and/or PARylation.

In support of this observation, we found that heat shock stress greatly reduces PARylation of mCherry-Golgin45, as shown in **Figure 4E**. While we did not detect any PARylation of control mCherry alone, mCherry-Golgin45-transfected sample showed very broad and intense bands with apparent molecular weight around ~80-90 kDa, which are slightly above expected mCherry-Golgin45 band typically at ~75 kDa. Strikingly, these intense bands almost disappeared completely after heat shock treatment for 2,4 and 6 hours, suggesting that TNKS1 modulation of Golgin45 stability is highly temperature sensitive (**Figure 4E**; compare lanes 2 and 3-5).

In order to investigate how heat shock stress may influence Golgin45 SUMOylation, HeLa cells were transfected with mCherry-Golgin45, myc-SUMO1 (or SUMO2 or SUMO3) and FLAG-tagged Ubc9 WT or DN overnight, followed by 43 ˚C heat shock for 1 hour. Cells were then lysed in RIPA buffer and subjected to western analysis. Unexpectedly, heat shock stress greatly increased SUMO2/3 modification (but not SUMO1 modification) on Golgin45 (**Figure 4F-H**; compare lanes 2 and 4), demonstrating that SUMO2/3 conjugation to Golgin45 may play more important roles in heat shock stress response,

whereas SUMO1 modification may be relevant to more housekeeping function of Golgin45 in the nucleus.

PML directly binds and facilitates SUMO2/3 conjugation to Golgin45, leading to Golgin45 inclusion into PML-NBs during heat shock response

Since Golgin45 was originally identified as a nuclear protein that is up-regulated during retinoid-induced maturation of NB4 promyelocytic leukaemia (PML) and our new results indicate that it appears to function as a stress response protein (*8, 13, 19*), we wondered whether SUMOylated Golgin45 may directly interact with PML and participate in the PML nuclear body formation and its function in genome maintenance during cellular stress.

As a preliminary study to survey interacting proteins of SUMOylated Golgin45, HeLa cells were co-transfected with mCherry-Golgin45 and with/without SUMO1 and Ubc9, followed by cell lysis in RIPA buffer and immunoprecipitation using anti-RFP antibody. We then analyzed the immunoprecipitates by proteomic analysis. The results showed that PML protein showed at least three-fold higher abundance in SUMOylated Golgin45 immunoprecipitates, compared to the control mCherry-Gol gin45 (**Figure 5A**).

To confirm this finding, HeLa cells were transfected with mCherry-Golgin45, followed by lysis in RIPA buffer and immunoprecipitation using anti-GRASP55, TNKS1 and PML protein, respectively. Western analysis of these immunoprecipitates confirmed that endogenous PML clearly interact with SUMOylated Golgin45, whereas neither GRASP55 immunoprecipitates nor TNKS1/2 immunoprecipitates pulled down SUMOylated Golgin45 (**Figure 5B**; compare upper bands in lane 3,4 and 5).

In support of this finding, we found that mCherry-Golgin45 pulls down significantly larger amount of endogenous PML and reduced amount of TNKS1 upon heat shock stress (**Figure 5C**). Importantly, we also observed that heat shock treatment induces greatly increased SUMO2/3 conjugation to various proteins overall, whereas there was no significant change in SUMO1 modification, which were reflected in increased higher MW upper bands in anti-SUMO2/3, but not in SUMO1 western blots. Taken together, these results further support the notion that heat shock stress greatly enhances Golgin45 SUMOylation by SUMO2/3 and reveal that heat shock stress increases Golgin45 SUMOylation and its binding to PML protein.

In order to study whether SUMOylated Golgin45 is a part of PML-NBs in the nucleus under heat shock stress, HeLa cells were transfected with mCherry-Golgin45 overnight, followed by 43 °C heat shock for 2 hours. Cells were then fixed and stained with anti-PML and GM130 antibodies and DAPI. Upon examining under confocal microscope, we found that mCherry-Golgin45 indeed co-localizes with the PML-NBs under heat shock stress, as shown **Figure 5D-E**. Unexpectedly, however, we found that over-expression SUMOylation-deficient Golgin45 8KR mutant significantly reduced the number of PML-NBs after heat shock treatment (**Figure 5D-E**), suggesting that the over-expressed 8KR mutant may function as a dominant negative for PML-NB formation.

These results were further validated using live cell imaging. To this end, cells were transfected with mCherry-Golgin45 or Golgin45-8KR mutant overnight, followed by live cell imaging using a confocal microscope for 2 hours under heat shock stress. These results were consistent with the earlier observation using fixed samples in that there was gradual and significant condensation of mCherry-Golgin45 WT into distinct puncta, while the 8KR mutant didn't show this condensation of red fluorescence during the 2 hours live cell imaging under heat shock condition (**Figure 5F**).

Finally, as PML was previously identified as a SUMO E3 ligase (*26*), the above results raised a possibility that PML may function as a SUMO E3 ligase for Golgin45. To test this hypothesis, we decided to knock down PML protein to see whether Golgin45 SUMOylation is affected. To this end, HeLa cells were treated with RNAi oligos against PML for 48 hours, followed by co-transfection with mCherry-Golgin45, myc-SUMO1 (or SUMO3) and FLAG-tagged Ubc9 WT or DN overnight.

Importantly, PML knockdown didn't have any influence on SUMO1 modification, but greatly decreased SUMO3 conjugation to mCherry-Golgin45, suggesting that PML may indeed function as a SUMO3-specific E3 ligase for Golgin45 (**Figure 5G-H**; compare lanes 2 and 4).

Discussion

In this study, we showed that a Golgi structural protein, Golgin45, is conjugated to SUMO1 under steady state condition, after it gets imported into the nucleus via its interaction with Importin-β2. Once in the nucleus, cellular stress (such as heat shock) likely further promotes SUMO2/3 conjugation to Golgin45 by PML as a SUMO E3-ligase, leading to its inclusion into PML-NBs, as shown in the schematic illustration (**Figure 6**). As noted in the introduction, Golgin45 is also a PARylated protein via its interaction with TNKS1 at the Golgi (*15*), and our new results indicate that this post-translational modification seems negatively regulated by Golgin45 SUMOylation (**Figure 2E**).

Several results support our hypothesis that Golgin45 may be a stress response protein. First, SUMO2/3 conjugation to Golgin45 is highly stimulated under heat shock stress (**Figure 4F-H**). Second, fractionation experiments indicate that SUMO3 conjugation to Golgin45 greatly increases nuclear import and/or retention of Golgin45 over SUMO1 modification (**Figure 4B**). Third, knockdown of PML protein selectively decreases SUMO3 conjugation to Golgin45, but not SUMO1 modification (**Figure 5E-F**), suggesting PML-SUMO2/3-Golgin45 as a novel stress response pathway, linking the Golgi and the nucleus.

A growing body of evidence has suggested that SUMO1 and SUMO2/3 may play distinct roles during stress response, in which SUMO2/3 provides a quick response to cellular stress. These include SUMOylation of NLRP3 during inflammatory response (*22, 27*), regulation of a non-canonical type I interferon response by SUMO2/3 (*28*) and differential effects of SUMO1 vs. SUMO3 on PKR activation (*21*), etc.

One of the limitations of the current study was that we were not able to detect SUMOylation of endogenous Golgin45. It is possible that the commercial polyclonal antibody used in our study does not recognize heavily SUMOylated Golgin45, especially considering the sheer size of SUMO being close to ~11 kDa and the number of SUMOylation reaching up to at least ~eight sites, which basically cover nearly half of entire Golgin45 protein (**Figure 1**). It is also difficult to rule out the possibility that SUMOylation of Golgin45 play more prominent roles in specific cell-types, such as neuronal cells or cells adapted for heavy secretory activity, which requires future studies.

Nevertheless, our results showed that exogenous over-expression of Golgin45 (8-KR), a SUMO-deficient mutant, greatly reduced the formation of PML-NBs under heat shock stress (**Figure 5D-F**). We don't

believe that these results indicate SUMOylated Golgin45 as an absolute requirement for PML-NB formation, but it does suggest that the SUMOylation-deficient Golgin45 mutant may function as a dominant negative for the nucleation of PML-NBs, which support the earlier observations by others (*29, 30*).

Why would a Golgi structural protein like Golgin45 get SUMOylated and function as a component of PML-NBs, influencing its assembly in the nucleus? Protein SUMOylation has been associated with cellular senescence via several senescence-related proteins, such as p53, TRF2 and SIRT1, etc, all of which are SUMOylated proteins (*31-36*). In this respect, it is worth noting that TNKS1 was originally identified as a PARP for TRF2 and its modulator in telomere maintenance (*37-39*).

Although it may be too speculative yet, these seeming connections point to a possibility that the dynamic interplay between Golgin45 SUMOylation and PARylation may be a part of a Golgi-derived feedback-loop, which is involved in regulation of stress-induced cellular senescence or genome maintenance pathway (*31*).

In support of this hypothesis, previous screening studies by others have shown that Histone Deacetylase-4 (HDAC4) may directly interact with both Golgin45 and TNKS1. Since HDAC4 is known to function as a SUMO E3 ligase for SIRT1 (*40*), our results suggest that more intricate network of post-translational modification-dependent inter-organelle communications may exist than was previously thought. In summary, we propose, based on our new results on PML-Golgin45-TNKS1 interplay, that SUMOylated Golgin45 may function to monitor and modulate cellular stress response by linking the Golgi and the nucleus.

Acknowledgement

Authors acknowledge Chengqian Zhang, Zhaomei Shi and Piliang Hao from Mass Spectrometry Core facility in School of Life Science and Technology, ShanghaiTech University, for technical support in LC-MS/MS and data analysis. Financial support of this study was provided by ShanghaiTech University.

Author Contributions

N.T and I.L initiated the project. Q.Y, X.Y and I.L designed the experiments. S.J, J.G, N.T, Y.D, L.Z, B.G, Q.Y, X.Y performed the experiments. Q.Y, X.Y and I.L wrote the manuscripts.

Declarations

The authors declare no conflict of interest.

Data availability statement All materials and data supporting this study are available from the corresponding authors (yuexh@shanghaitech.edu; qianyi@shanghaitech.edu; leeintaek@shanghaitech.edu) upon reasonable request

References

1. A. B. Celen, U. Sahin, Sumoylation on its 25th anniversary: mechanisms, pathology, and emerging concepts. *FEBS J* **287**, 3110-3140 (2020).
2. I. A. Hendriks, A. C. Vertegaal, A comprehensive compilation of SUMO proteomics. *Nat Rev Mol Cell Biol* **17**, 581-595 (2016).
3. R. T. Hay, Decoding the SUMO signal. *Biochem Soc Trans* **41**, 463-473 (2013).
4. M. Sundvall, Role of Ubiquitin and SUMO in Intracellular Trafficking. *Curr Issues Mol Biol* **35**, 99-108 (2020).
5. R. Geiss-Friedlander, F. Melchior, Concepts in sumoylation: a decade on. *Nat Rev Mol Cell Biol* **8**, 947-956 (2007).
6. A. Flotho, F. Melchior, Sumoylation: a regulatory protein modification in health and disease. *Annu Rev Biochem* **82**, 357-385 (2013).
7. A. Pichler, C. Fatouros, H. Lee, N. Eisenhardt, SUMO conjugation - a mechanistic view. *Biomol Concepts* **8**, 13-36 (2017).
8. M. A. Maroui *et al.*, Promyelocytic Leukemia Protein (PML) Requirement for Interferon-induced Global Cellular SUMOylation. *Mol Cell Proteomics* **17**, 1196-1208 (2018).
9. U. Sahin, H. de The, V. Lallemand-Breitenbach, PML nuclear bodies: assembly and oxidative stress-sensitive sumoylation. *Nucleus* **5**, 499-507 (2014).
10. U. Sahin *et al.*, Oxidative stress-induced assembly of PML nuclear bodies controls sumoylation of partner proteins. *J Cell Biol* **204**, 931-945 (2014).
11. U. Patra, S. Muller, A Tale of Usurpation and Subversion: SUMO-Dependent Integrity of Promyelocytic Leukemia Nuclear Bodies at the Crossroad of Infection and Immunity. *Front Cell Dev Biol* **9**, 696234 (2021).
12. R. S. Glingston, R. Deb, S. Kumar, S. Nagotu, Organelle dynamics and viral infections: at cross roads. *Microbes Infect* **21**, 20-32 (2019).
13. H. R. Chang *et al.*, The functional roles of PML nuclear bodies in genome maintenance. *Mutat Res* **809**, 99-107 (2018).

14. M. Scherer, T. Stamminger, Emerging Role of PML Nuclear Bodies in Innate Immune Signaling. *J Virol* **90**, 5850-5854 (2016).
15. X. Yue *et al.*, Tankyrase-1-mediated degradation of Golgin45 regulates glycosyltransferase trafficking and protein glycosylation in Rab2-GTP-dependent manner. *Commun Biol* **4**, 1370 (2021).
16. S. Pellegrino, M. Altmeyer, Interplay between Ubiquitin, SUMO, and Poly(ADP-Ribose) in the Cellular Response to Genotoxic Stress. *Front Genet* **7**, 63 (2016).
17. B. Short *et al.*, A GRASP55-rab2 effector complex linking Golgi structure to membrane traffic. *J Cell Biol* **155**, 877-883 (2001).
18. A. Gartner *et al.*, Acetylation of SUMO2 at lysine 11 favors the formation of non-canonical SUMO chains. *EMBO Rep* **19**, (2018).
19. E. Duprez *et al.*, JEM-1, a novel gene encoding a leucine-zipper nuclear factor upregulated during retinoid-induced maturation of NB4 promyelocytic leukaemia. *Oncogene* **14**, 1563-1570 (1997).
20. D. Dormann *et al.*, ALS-associated fused in sarcoma (FUS) mutations disrupt Transportin-mediated nuclear import. *EMBO J* **29**, 2841-2857 (2010).
21. G. Maarifi, F. El Asmi, M. A. Maroui, L. Dianoux, M. K. Chelbi-Alix, Differential effects of SUMO1 and SUMO3 on PKR activation and stability. *Sci Rep* **8**, 1277 (2018).
22. R. Barry *et al.*, SUMO-mediated regulation of NLRP3 modulates inflammasome activity. *Nat Commun* **9**, 3001 (2018).
23. J. Karhausen, L. Ulloa, W. Yang, SUMOylation Connects Cell Stress Responses and Inflammatory Control: Lessons From the Gut as a Model Organ. *Front Immunol* **12**, 646633 (2021).
24. P. Novick, R. Schekman, Secretion and cell-surface growth are blocked in a temperature-sensitive mutant of Saccharomyces cerevisiae. *Proc Natl Acad Sci U S A* **76**, 1858-1862 (1979).
25. C. E. Gilbert, E. Sztul, C. E. Machamer, Commonly used trafficking blocks disrupt ARF1 activation and the localization and function of specific Golgi proteins. *Mol Biol Cell* **29**, 937-947 (2018).
26. Y. Chu, X. Yang, SUMO E3 ligase activity of TRIM proteins. *Oncogene* **30**, 1108-1116 (2011).
27. L. Shao *et al.*, SUMO1 SUMOylates and SENP3 deSUMOylates NLRP3 to orchestrate the inflammasome activation. *FASEB J* **34**, 1497-1515 (2020).
28. J. T. Crowl, D. B. Stetson, SUMO2 and SUMO3 redundantly prevent a noncanonical type I interferon response. *Proc Natl Acad Sci U S A* **115**, 6798-6803 (2018).
29. H. Takahashi, S. Hatakeyama, H. Saitoh, K. I. Nakayama, Noncovalent SUMO-1 binding activity of thymine DNA glycosylase (TDG) is required for its SUMO-1 modification and colocalization with the promyelocytic leukemia protein. *J Biol Chem* **280**, 5611-5621 (2005).
30. S. Weger, E. Hammer, M. Engstler, The DNA topoisomerase I binding protein topors as a novel cellular target for SUMO-1 modification: characterization of domains necessary for subcellular localization and sumolation. *Exp Cell Res* **290**, 13-27 (2003).
31. A. Princz, N. Tavernarakis, The role of SUMOylation in ageing and senescent decline. *Mech Ageing Dev* **162**, 85-90 (2017).
32. L. Ivanschitz *et al.*, PML IV/ARF interaction enhances p53 SUMO-1 conjugation, activation, and senescence. *Proc Natl Acad Sci U S A* **112**, 14278-14283 (2015).
33. M. Gostissa *et al.*, Activation of p53 by conjugation to the ubiquitin-like protein SUMO-1. *EMBO J* **18**, 6462-6471 (1999).
34. M. Campagna *et al.*, SIRT1 stabilizes PML promoting its sumoylation. *Cell Death Differ* **18**, 72-79 (2011).
35. D. Churikov *et al.*, SUMO-Dependent Relocalization of Eroded Telomeres to Nuclear Pore Complexes Controls Telomere Recombination. *Cell Rep* **15**, 1242-1253 (2016).

36. J. Her, Y. Y. Jeong, I. K. Chung, PIAS1-mediated sumoylation promotes STUbL-dependent proteasomal degradation of the human telomeric protein TRF2. *FEBS Lett* **589**, 3277-3286 (2015).
37. S. Smith, I. Giriat, A. Schmitt, T. de Lange, Tankyrase, a poly(ADP-ribose) polymerase at human telomeres. *Science* **282**, 1484-1487 (1998).
38. B. van Steensel, A. Smogorzewska, T. de Lange, TRF2 protects human telomeres from end-to-end fusions. *Cell* **92**, 401-413 (1998).
39. S. Smith, T. de Lange, Tankyrase promotes telomere elongation in human cells. *Curr Biol* **10**, 1299-1302 (2000).
40. X. Han *et al.*, HDAC4 stabilizes SIRT1 via sumoylation SIRT1 to delay cellular senescence. *Clin Exp Pharmacol Physiol* **43**, 41-46 (2016).

Materials and Methods

Reagents and Antibodies

All common reagents were purchased from Sigma-Aldrich, unless otherwise mentioned. XAV939 (S1180), MG132 (S2619), TAK981 (S8341), TAK243 (S8829), Doxorubicin (S1208), Torin1 (S2827) and Importazole (S8446) were purchased from Selleck. Cycloheximide (100mM) from Yeasen (40325ES03). Leptomycin B from Beyotime Biotechnology (S1726). The following antibodies were used : rabbit polyclonal anti-PML (21041-1-AP, proteintech), rabbit polyclonal anti-mCherry (ab167453, Abcam), mouse monoclonal anti-FLAG (F1804, Sigma-Aldrich), rabbit anti-Myc (2278S, Cell Signaling Technology), mouse anti-Actin (3700s, Cell Signaling Technology), anti-GST (RPN1236, Cytiva), rabbit polyclonal anti-Mono-ADP Ribose (83732S, Cell Signaling Technology), rabbit polyclonal anti-Golgin45 (PA5-30714, Thermo), anti-ACBD3 (HPA015594, Sigma Aldrich), mouse monoclonal anti-GRASP55 (ab211532, Abcam), anti-GAPDH (KC-5G5, Kangchen Bio-tech), mouse monoclonal anti-Transportin 1 (ab10303, Abcam), rabbit polyclonal anti-Lamin B (12987-1-AP, Proteintech), mouse monoclonal anti-Tankyrase1/2 (sc-365897, Santa Cruz), mouse anti-HA-Tag (2367s, Cell Signaling Technology). Anti-Rabbit Alexa Fluor 488 (A21441), Alexa Fluor 568 (A10042), Alexa Fluor 647 (A21245) and anti-Mouse Alexa Fluor 488 (A21200), Alexa Fluor 568 (A10037), Alexa Fluor 647 (A21236) for Immunofluorescence were obtained from ThermoFisher. All siRNA oligos were custom designed by Ribobiology. The sequence of the non-targeting control siRNA was UUCUCCGAACGUGUCACGU. Human PML siRNA #1: CGCCCUGGAUAACGUCUUU.

Cell culture and and transfection

HeLa (ATCC, CCL-2) cells were grown in DMEM supplemented with 10% FBS (Thermo) and U-2 OS (Stem Cell Bank, Chinese Academy of Sciences) were grown in McCoy's 5A Medium supplemented with 10%

FBS at 37 °C. Transfection of DNA constructs and siRNAs was performed using Lipofectamine 2000 and RNAiMAX (ThermoFisher), respectively, according to the manufacturer's instructions. For DNA expression, cells were transfected 24 hours before Co-IP experiments and 18 hours for IF experiments. For siRNA knockdown, cells were transfected 72 hours before experiments.

Co-immunoprecipitation (Co-IP) and Immunoblotting

For Co-IP experiments, total lysates were prepared using lysis buffer (25mM HEPES, pH 7.4, 100mM NaCl, 1% NP-40, 1× protease inhibitor cocktail (Roche)). Subsequently, the total lysates were passed through a syringe needle (15 times) and then incubated at 4°C with end-over-end agitation for 1 hour. The lysates were then cleared by centrifugation at 15,000 x g for 20 min. The supernatants were incubated with indicated antibodies and protein G agarose beads (L00209, GenScript) for 4 hours at 4°C with end-over-end agitation. The beads were washed two times with ice-cold lysis buffer and one time with PBS. Proteins were eluted by boiling in 2× SDS running buffer and subjected to SDS-PAGE for immunoblotting.

For immunoblotting, proteins were separated by SDS-PAGE (Genscript) and transferred onto nitrocellulose membranes (Amersham). Membranes were probed with specific primary antibodies and then with peroxidase-conjugated secondary antibodies (Jackson ImmunoResearch). The bands were visualized with chemiluminescence (Clarity Western ECL Substrate, Bio-Rad) and imaged by a ChemiDoc Touch imaging system (Bio-Rad).

Immunofluorescence staining

Cells grown on glass coverslips in 24-well plates or glass bottom 24-well plates (P24-1.5H-N, Cellvis) were fixed for 10 min with 4% paraformaldehyde (PFA), permeabilized in permeabilization Buffer (0.3% Igepal CA-630, 0.05% Triton-X 100, 0.1% IgG-free BSA in PBS) for 5 min, and blocked in blocking buffer (0.05% Igepal CA-630, 0.05% Triton-X 100, 5% normal goat serum in PBS) for 60 min. Primary and secondary antibodies were applied in blocking buffer for 1 hour. The nucleus was stained with Hoechst-33342 (sc-200908, Santa cruz Biotechnology). Cells were washed three times with wash buffer (0.05% Igepal CA-630, 0.05% Triton-X 100, 0.2% IgG-free BSA in PBS) and twice with PBS. Coverslips were mounted using ProLong Gold Antifade Reagent (ThermoFisher). Dip coverslip in diH2O before mounting to prevent salt contamination. Images were acquired with a Zeiss LSM880 confocal microscope using a 63× Apochromat oil-immersion objective.

Live cell imaging

For live cell imaging of mCherry-Golgin45 or 8-KR mutant, HeLa cells were seeded on a glass-bottom dish (35-mm diameter, Cellvis) coated with fibronectin (Millipore). After 18-h transfection, cells were imaged with a 100× objective on a Perkin Elmer UltraVIEW Spinning disk confocal microscope at 43°C. Images were acquired every 5 min for 2 hours.

CRISPR/Cas9 gene editing

Gene-specific single-guide RNA (sgRNA) sequences were designed using the online software (http://crispr.mit.edu) resource from the Zhang Laboratory and were cloned into pSpCas9(BB)-2A-GFP (Addgene 48138) using the BbsI restriction enzyme sites. The target sequence was as follows: Golgin45 sgRNA, gttacttcatccccaatccgagg. The single-guide RNA DNA sequence was cloned into the pSpCas9(BB)-2A-GFP plasmid. U-2 OS cells were transfected with Golgin45 sgRNA-containing plasmid. After two days, isolation of clonal cell populations was performed by dilution into 96-well plate. Single clones were expanded and screened by immunoblotting, genomic sequencing, and functional assays.

Lentivirus preparation and infection

To produce lentivirus, a lentiviral vector containing mCherry-Goglin45, mCherry-Golgin45 8-KR mutant, mCherry-Golgin45 R375A mutant along with packing (psPAX2) and envelop (pMD2.G) vectors were transfected into 293FT cells using Lipofectamine 2000. The supernatants were collected after transfection for 48 hr and 72 hr, filtrated with 0.45 nm filters, and concentrated using Lenti-concentration kit (AC04L441, life-ilab). Resuspended viral pellets were used to infect cells in the presence of polybrene.

Subcellular Protein Fractionation

To produce subcellular fractionation, a cell subcellular fractionation kit (P0027 , beyotime) was used. Briefly, cells were washed twice and lysed in buffer A plus 1mM PMSF. The lysates was incubate at ice for 15 min. After incubation, buffer B was add to lysates and incubate at ice for 1 min. Then lysates was vortex 5s and then centrifuged at 4°C for 5 min at 16,000 g. Supernatants were collected as cytoplasmic extracts, and pellets were collected as nuclear extrats. Equal amounts of cytoplasmic and nuclear extracts were subjected to western blot.

Cycloheximide chase assay

The stability of Golgin45 was determined by cycloheximide chase assays. HeLa or U-2 OS cells were seeded in six-well plates (Nest), or cells were transiently transfected with mCherry-Golgin45, mCherry-Golgin45 8-KR mutant, mCherry-Golgin45 ΔTBD, mCherry-Golgin45-K350/370/371R mutant for 18 h. Cells were treated with cycloheximide (50 μg/ml) for the indicated times and then collected and lysed by Western blotting.

QUANTIFICATION AND STATISTICAL ANALYSIS

Quantification of PML-NB number or mCherry-Golgin45 protein levels relative to β-actin expression were done using Fiji. All data were analyzed using the Prism GraphPad software (version 9.0) and statistical analysis was performed using one-way ANOVA with a Tukey's post-hoc test (n.s., not significant; *, $p < 0.05$; **, $p < 0.01$; ***, $p < 0.001$; ****, $p < 0.0001$). Data are presented as mean ± SD. All experiments were carried out in triplicates, unless specified otherwise.

GST Pulldown Assay

200μg GST-fusion proteins were immobilized on glutathione Sepharose 4B (GE Healthcare) for each sample. The resins were washed 3 times with PBS+0.5% Trition-X100 and then incubated with 0.1μM Importin β2 proteins in pulldown buffer (25mM Hepes, pH 7.37, 300mM NaOAc, 25mM Mg(OAc)2, 0.5% Triton X-100, 1mM DTT and protease inhibitors, 500μl total volumn for each reaction) at 4°C for 2hrs. The resins were washed 4 times with pulldown buffer. Samples were prepared by resuspension of the resins with 2x SDS loading buffer in 95°C.

Figure Legends

Fig.1 Golgin45 is subjected to SUMO1/3 modification (A) Endogenous Golgin45 expression was downregulated after TAK981 treatment. Hela cells were treated with 5 μM XAV939 or 10 μM TAK981 for different time points. Cells were harvested for western blot using indicated antibodies. (B) Hela cells were treated with different concentration of TAK981 for 24 hours. Cells were harvested for western blot using indicated antibodies. (C) Golgin45 is robustly conjugated to SUMO1 and the SUMOylation of Golgin45 is abolished by a SUMO-activating enzyme (SAE) inhibitor TAK981. Hela cells were transiently transfected with the indicated plasmids overnight, then the cells were treated with DMSO or 10 μM TAK981 for 8 hours and then SUMO1-modified Golgin45 was analyzed by western blot. (D) Golgin45 is SUMOylated by both SUMO1 and SUMO3. Hela cells were transfected with myc-SUMO1/3, Flag-UBC9-WT or its dominant-negative (DN) mutation and mCherry-Golgin45 for 18 hours, then the cells were lysed and SUMOylation of Golgin45 was examined by western blot. (E) The SUMOylation sites modified by SUMO1 lie within the N terminal of Golgin45. Hela cells were transfected with mCherry-Golgin45 (121-400) (N terminal deleted truncation) or mCherry-Golgin45 (1-400) (full length) with myc-SUMO1 and Flag-UBC9 for 18 hours, the mCherry-Golgin45 SUMOylation was analyzed by western blot. (F) Golgin45 is SUMOylated at multiple sites. Hela cells were transfected with the indicated plasmids for 18 hours. Cells were lysed and analyzed by western blotting using anti-mCherry, anti-Flag and anti-Myc. (G) Schematic of Golgin45 domains, showing the identified SUMO acceptor sites and predicted ubiquitination sites. TBD, Tankyrase binding domain; CC, Coiled-coil domain. (H) Mutation of the 8 SUMOylation sites (8-KR) significantly reduces the Golgin45 SUMOylation modified by SUMO1 or SUMO2/3. (I-J) Hela cells were transfected with the indicated plasmids for 18 hours. Cells were lysed and analyzed by western blotting. Representative blots are shown and experiments were repeated three

times.

Fig.2 SUMOylation enhances Golgin45 protein stability by inhibiting TNKS1-dependent PARylation of Golgin45 (A) XAV939 treatment increases SUMOylation on Golgin45. HeLa cells were transiently transfected with mCherry-Golgin45 and SUMO1 along with Ubc9 WT or DN, followed by either DMSO or XAV939 (a specific inhibitor of TNKS1/2). The cells were lysed and analyzed by western blotting using antibodies against the indicated proteins. (B-C) Deletion of TNKS1 binding domain (ΔTBD) increases both SUMO1 and SUMO3 modified SUMOylation of Golgin45. After transfection with the indicate plasmids, HeLa cells were lysed and analyzed by western blotting using antibodies against the indicated proteins. (D) HeLa cells expressing mCherry-Golgin45, mCherry-Golgin45-8KR mutant were treated with cycloheximide (50μg/ml) for the indicated times. Ectopically expressed WT and mutant mCherry-Golgin45 protein levels were monitored by immunoblotting. Quantification of exogenous protein levels relative to β-actin expression is shown. (E) SUMOylation of mCherry-Golgin45 inhibits its PARylation. Hela cells transfected with indicate plasmids were lysed and immunoprecipitated using anti-RFP beads, and blotted with either anti-mCherry or anti-PAR. (F) Golgin45 PARylation is increased for Golgin45 8-KR mutant. HeLa cells expressing GST, GST-Golgin45 or GST-Golgin45-8KR were lysed and pulled down using GST beads, and analyzed by western blotting using anti-GST or anti-PAR antibodies. Representative blots are shown and experiments were repeated three times.

Fig.3 Importin-β2-mediated nuclear import of Golgin45 plays an important role in Golgin45 SUMOylation (A) Domain structure of Golgin45. Tankyrase-1, Rab2-GTP, and GRASP55 bind to the N-terminus, coiled coil domain, and the C-terminus of Golgin45, respectively. The putative NLS on Golgin45 for importin β2 is noted with an arrow indicating a key residue R375. (B) R375A mutation greatly reduced the binding between Importin β2 and Golgin45. Purified His-tagged importin β2 was incubated with GST, GST-Golgin45 336-385 and GST-Golgin45 336-385 R375A and the bound fractions were analyzed by western blots using anti-importin β2 antibody. (C) Importin β2 was co-immunoprecipitated by Golgin45, but not R375A mutant. HeLa cells were tranfected with mCherry, mCherry-Golgin45 (mCh-G45), or mCherry-Golgin45 R375A (mCh-G45 R375A) for 18 h. Cells were lysed, incubated with anti-RFP beads, and analyzed with indicated antibodies. (D) mCherry-Golgin45, but not the R375A mutant, localized to the nucleus. HeLa cells overexpressing mCherry-Golgin45 or mCherry-Golgin45 R375A were fixed and stained with anti-GM130 antibody. Images were acquired using Zeiss LSM880 confocal microscope. (E) Statistical analysis was performed by one-way ANOVA to quantify the

fluorescent intensity ratio of nucleus-localized Golgin45 over the total mCherry-Golgin45. (F-G) R375A mutation decreases SUMOylation of Golgin45. HeLa cells expressing mCherry-Golgin45, mCherry-Golgin45-VA mutant, mCherry-Golgin45-S15D mutant or mCherry-Golgin45-R375 mutant with SUMO1 (F) or SUMO3 (G) and UBC9 were lysed and SUMOylation of Golgin45 were analyzed by western blotting.

Fig.4 Heat shock stress increases protein level and SUMOylation of Golgin45. (A-B) HeLa cells expressing myc-SUMO1 (A) or SUMO3 (B) Flag-UBC9-WT or DN mutation and mCherry-Golgin45 were subjected to subcellular fractionation. The levels of SUMOylatd Golgin45 in nuclear and cytoplasmic fractions were determined by immunoblotting with anti-mCherry antibody. The relative purity of the nuclear and cytoplasmic fractions was confirmed by sequential probing for the nuclear marker lamin B and the cytoplasmic marker GAPDH. W, whole cell lysate; C, cytoplasm; N, nucleus. (C) Heat shock increases nuclear localization of Golgin45. HeLa cells expressing mCherry or mCherry-Golgin45 were treated with heat shock (HS) or no heat shock (NHS) for 1h, and then subjected to subcellular fractionation. The levels of Golgin45 in nuclear and cytoplasmic fractions were determined by immunoblotting with anti-mCherry antibody. (D) Heat shock increases endogenous protein level of Golgin45. HeLa cells were treated with heat shock for the indicated time points and harvested for western blots using indicated antibodies. (E) Heat shock inhibits PARylation of Golgin45. HeLa cells expressing mCherry or mCherry-Golgin45 were treated with heat shock for indicated time points. Then cells were lysed and immunoprecipitated using anti-RFP beads and blotted with either anti-mCherry or anti-PAR antibodies. (F-H) Heat shock increases SUMO2/3 modified SUMOylation of Golgin45. HeLa cells expressing myc-SUMO1(F), SUMO2(G) or SUMO3(H), Flag-UBC9-WT or DN mutation and mCherry-Golgin45 were treated with or without heat shock for 1h. Cells were harvested for western blots using indicated antibodies.

Fig.5 Heat shock stress increases SUMOylation of Golgin45 and promotes its inclusion into PML nuclear bodies. (A) Volcano plot representing results of the label-free IP-MS of SUMOylated mCherry-Golgin45. The logarithmic ratio of protein intensities in the SUMOylated mCherry-Golgin45 /mCherry-Golgin45-CoIP were plotted against negative logarithmic p-values of the t test performed from the triplicates. Indicated are known or candidate binding partners (red). (B) PML forms a complex with both SUMOylated and non-SUMOylated Golgin45. The protein extracts from HeLa cells expressing myc-SUMO1, HA-UBC9-WT and mCherry-Golgin45 were immunoprecipitated with anti-GRASP55, anti-

Tankyrase1/2 or anti-PML antibodies. These lysates and the immunoprecipitates were analyzed by western blotting using anti-mCherry antibody and antibodies against the indicated proteins. (C) HeLa cells expressing mCherry-Golgin45 were treared with or without heat shock. The protein extracts were immunoprecipitated with anti-IgG or anti-RFP beads. These lysates and the immunoprecipitates were analyzed by western blotting using antibodies against the indicated proteins. (D) HeLa cells expressing mCherry-Golgin45 were treated with heat shock (HS) or no heat shock (NHS) for 2h. Cells were then fixed and stained with anti-PML and anti-GM130 antibodies and DAPI. Scale bar, 10 μm. (E) Number of PML-NB per nucleus in (D) was quantified. Statistical analysis was performed using one-way ANOVA with a Tukey's post-hoc test (*, $p < 0.05$; ****, $p < 0.0001$). N=30 cells. (F) HeLa cells expressing mCherry-Golgin45 WT or 8-KR mutant were monitored by live cell imaging acquired every 5 min for 2 hours at 43°C. Imaging sequences at the indicated time points are presented here. Scale bars = 14 μm. (G-H) HeLa cells were treated with control siRNA or RNAi oligos against PML for 48 hours, followed by co-transfection with mCherry-Golgin45, myc-SUMO1 (or SUMO3) and FLAG-tagged Ubc9 WT or DN overnight. Cells were lysed and SUMOylation of Golgin45 were analyzed by western blotting.

Fig.6 Model for Golgin45 SUMOylation and its role in cellular stress response. Golgin45 gets imported into the nucleus via its interaction with Importin-β2. Golgin45 is conjugated to SUMO1 under steady state condition. Cellular stress (such as heat shock) promotes SUMO2/3 conjugation to Golgin45 by PML as a SUMO E3-ligase, leading to its inclusion into PML-NBs.

Supplementary Figure 1 HeLa cells were transiently transfected with the indicated plasmids overnight, then the cells were treated with DMSO, Glucose depletion, 500 nM Doxorubicin, 200 nM Torin1, 10 μM TAK243, 10 μM TAK981 or 20 μM TBHQ for 8 hours and then SUMO1-modified Golgin45 was analyzed by western blot.

Supplementary Figure 2 Golgin45 TBD deletion mutation or potential ubiquitination sites mutation increases protein stability of Golgin45. HeLa cells expressing mCherry-Golgin45, mCherry-Golgin45-K350/370/371R or mCherry-Golgin45-△TBD mutant were treated with cycloheximide (50μg/ml) for the indicated times. Ectopically expressed WT and the mutant mCherry-Golgin45 protein levels were monitored by immunoblotting. Quantification of mCherry-Golgin45 protein levels relative to GAPDH expression are shown in the graph to the right.

Figure 1

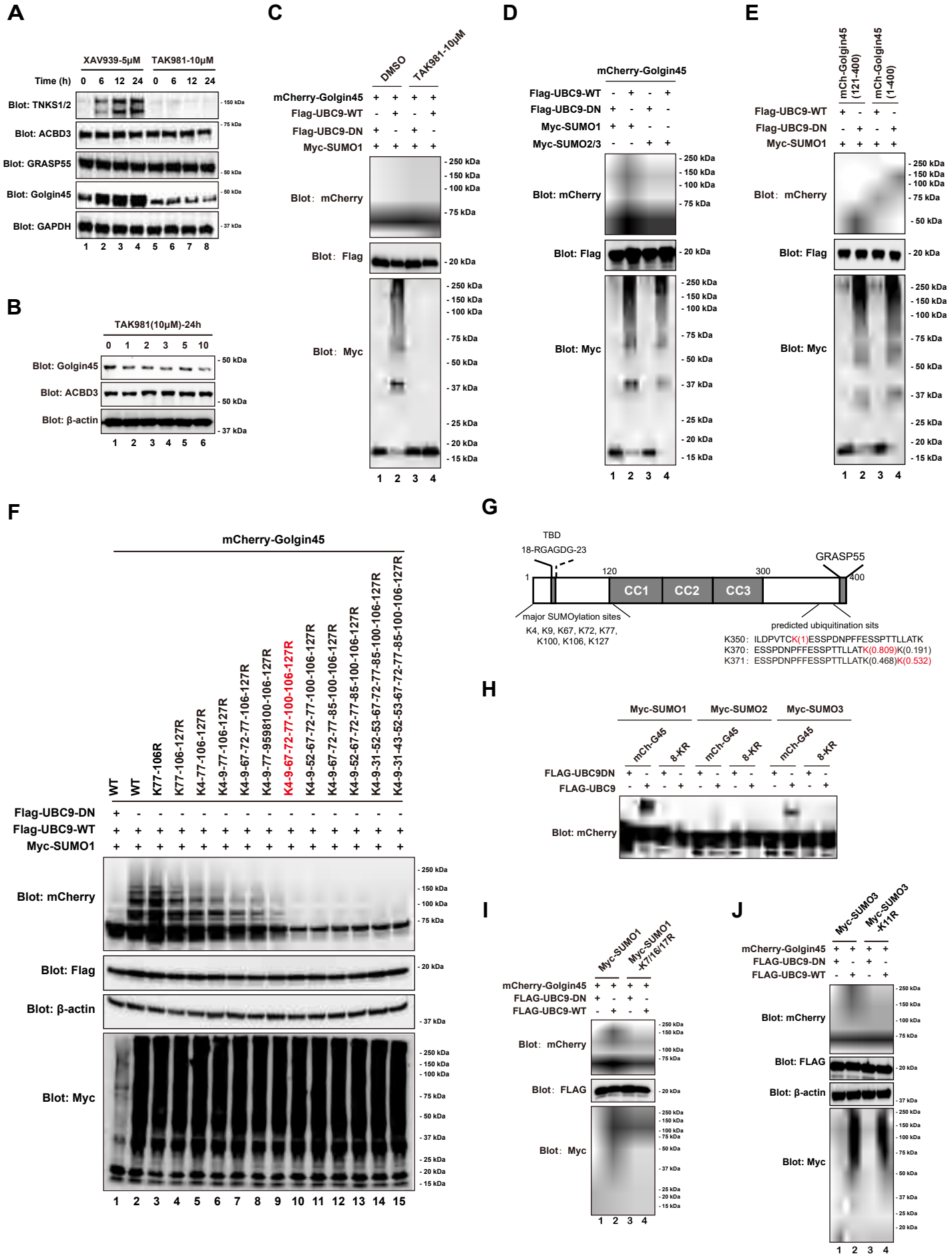
A
XAV939-5μM
TAK981-10μM
Time (h) 0 6 12 24 0 6 12 24
Blot: TNKS1/2
Blot: ACBD3
Blot: GRASP55
Blot: Golgin45
Blot: GAPDH
1 2 3 4 5 6 7 8
B
TAK981(10μM)-24h
0 1 2 3 5 10
Blot: Golgin45
Blot: ACBD3
Blot: β-actin
1 2 3 4 5 6
C
DMSO
TAK981-10μM
mCherry-Golgin45
Flag-UBC9-WT
Flag-UBC9-DN
Myc-SUMO1
Blot: mCherry
Blot: Flag
Blot: Myc
1 2 3 4
D
mCherry-Golgin45
Flag-UBC9-WT
Flag-UBC9-DN
Myc-SUMO1
Myc-SUMO2/3
Blot: mCherry
Blot: Flag
Blot: Myc
1 2 3 4
E
mCh-Golgin45 (121-400)
mCh-Golgin45 (1-400)
Flag-UBC9-WT
Flag-UBC9-DN
Myc-SUMO1
Blot: mCherry
Blot: Flag
Blot: Myc
1 2 3 4
F
mCherry-Golgin45
WT
WT
K77-106R
K77-106-127R
K4-77-106-127R
K4-9-77-106-127R
K4-9-67-72-77-106-127R
K4-9-77-9598100-106-127R
K4-9-67-72-77-100-106-127R
K4-9-52-67-72-77-100-106-127R
K4-9-67-72-77-85-100-106-127R
K4-9-52-67-72-77-85-100-106-127R
K4-9-31-52-53-67-72-77-85-100-106-127R
K4-9-31-43-52-53-67-72-77-85-100-106-127R
Flag-UBC9-DN
Flag-UBC9-WT
Myc-SUMO1
Blot: mCherry
Blot: Flag
Blot: β-actin
Blot: Myc
1 2 3 4 5 6 7 8 9 10 11 12 13 14 15
G
TBD
18-RGAGDG-23
GRASP55
1
120
300
400
CC1
CC2
CC3
major SUMOylation sites
K4, K9, K67, K72, K77, K100, K106, K127
predicted ubiquitination sits
K350: ILDPVTCK(1)ESSPDNPFFESSPTTLATK
K370: ESSPDNPFFESSPTTLLATK(0.809)K(0.191)
K371: ESSPDNPFFESSPTTLLATK(0.468)K(0.532)
H
Myc-SUMO1
Myc-SUMO2
Myc-SUMO3
mCh-G45
8-KR
FLAG-UBC9DN
FLAG-UBC9
Blot: mCherry
I
Myc-SUMO1
Myc-SUMO1 -K7/16/17R
mCherry-Golgin45
FLAG-UBC9-DN
FLAG-UBC9-WT
Blot: mCherry
Blot: FLAG
Blot: Myc
1 2 3 4
J
Myc-SUMO3
Myc-SUMO3 -K11R
mCherry-Golgin45
FLAG-UBC9-DN
FLAG-UBC9-WT
Blot: mCherry
Blot: FLAG
Blot: β-actin
Blot: Myc
1 2 3 4

Figure 2

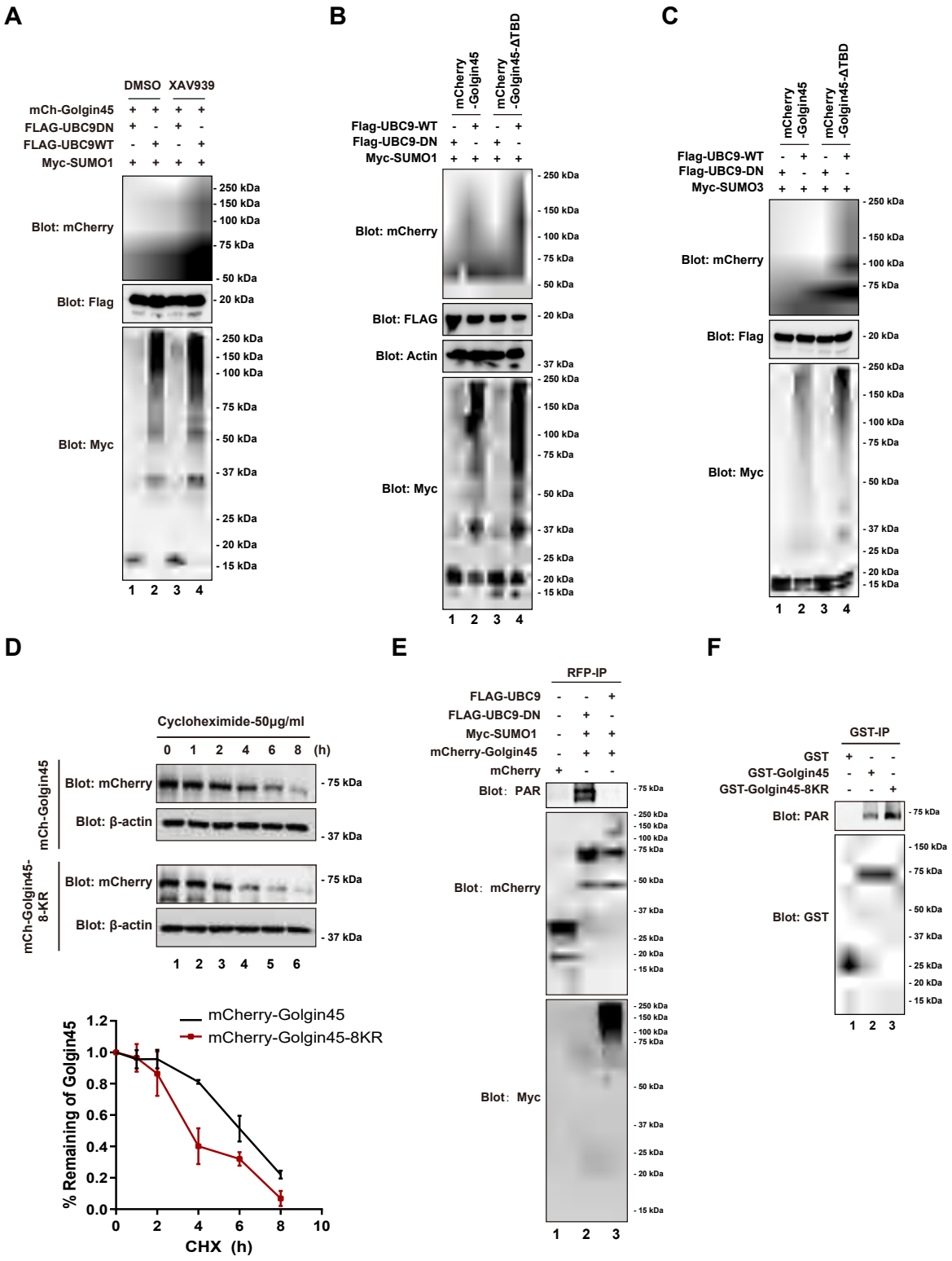
A
DMSO XAV939
mCh-Golgin45 + + + +
FLAG-UBC9DN + - + -
FLAG-UBC9WT - + - +
Myc-SUMO1 + + + +
Blot: mCherry
Blot: Flag
Blot: Myc
250 kDa
150 kDa
100 kDa
75 kDa
50 kDa
37 kDa
25 kDa
20 kDa
15 kDa
1 2 3 4
B
mCherry -Golgin45
mCherry -Golgin45-ΔTBD
Flag-UBC9-WT - + - +
Flag-UBC9-DN + - + -
Myc-SUMO1 + + + +
Blot: mCherry
Blot: FLAG
Blot: Actin
Blot: Myc
C
mCherry -Golgin45
mCherry -Golgin45-ΔTBD
Flag-UBC9-WT - + - +
Flag-UBC9-DN + - + -
Myc-SUMO3 + + + +
Blot: mCherry
Blot: Flag
Blot: Myc
D
Cycloheximide-50μg/ml
0 1 2 4 6 8 (h)
mCh-Golgin45
mCh-Golgin45-8-KR
Blot: mCherry
Blot: β-actin
1 2 3 4 5 6
mCherry-Golgin45
mCherry-Golgin45-8KR
% Remaining of Golgin45
CHX (h)
E
RFP-IP
FLAG-UBC9 - - +
FLAG-UBC9-DN - + -
Myc-SUMO1 - + +
mCherry-Golgin45 - + +
mCherry + - -
Blot: PAR
Blot: mCherry
Blot: Myc
1 2 3
F
GST-IP
GST + - -
GST-Golgin45 - + -
GST-Golgin45-8KR - - +
Blot: PAR
Blot: GST
1 2 3

Figure 3

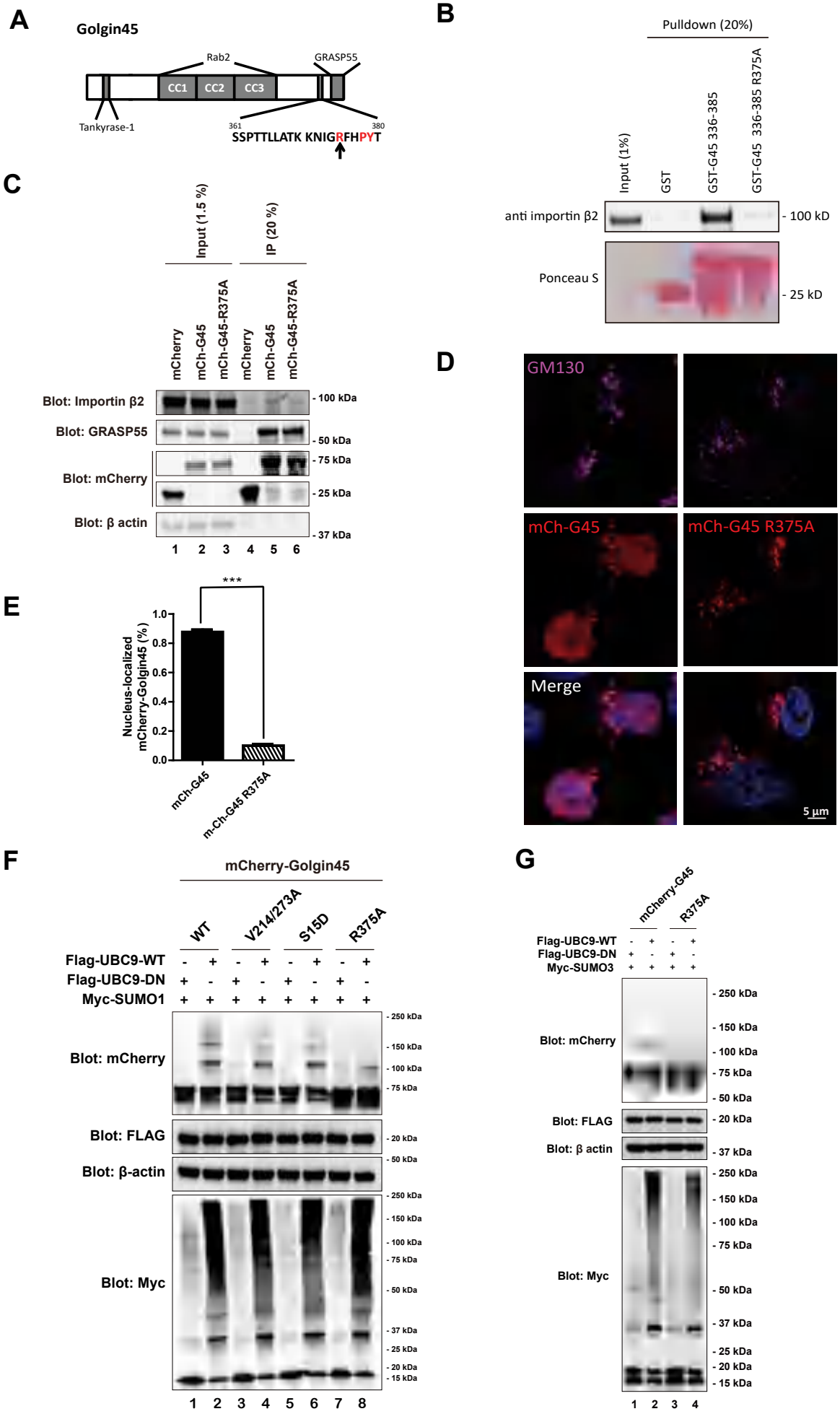
A
Golgin45
Rab2
GRASP55
CC1
CC2
CC3
Tankyrase-1
361
380
SSPTTLLATK KNIGRFHPYT
B
Pulldown (20%)
Input (1%)
GST
GST-G45 336-385
GST-G45 336-385 R375A
anti importin β2
- 100 kD
Ponceau S
- 25 kD
C
Input (1.5 %)
IP (20 %)
mCherry
mCh-G45
mCh-G45-R375A
mCherry
mCh-G45
mCh-G45-R375A
Blot: Importin β2
- 100 kDa
Blot: GRASP55
- 50 kDa
- 75 kDa
Blot: mCherry
- 25 kDa
Blot: β actin
- 37 kDa
1 2 3 4 5 6
D
GM130
mCh-G45
mCh-G45 R375A
Merge
5 µm
E
***
Nucleus-localized mCherry-Golgin45 (%)
1.0
0.8
0.6
0.4
0.2
0.0
mCh-G45
m-Ch-G45 R375A
F
mCherry-Golgin45
WT
V214/273A
S15D
R375A
Flag-UBC9-WT - + - + - + - +
Flag-UBC9-DN + - + - + - + -
Myc-SUMO1 + + + + + + + +
Blot: mCherry
- 250 kDa
- 150 kDa
- 100 kDa
- 75 kDa
Blot: FLAG
- 20 kDa
Blot: β-actin
- 50 kDa
Blot: Myc
- 250 kDa
- 150 kDa
- 100 kDa
- 75 kDa
- 50 kDa
- 37 kDa
- 25 kDa
- 20 kDa
- 15 kDa
1 2 3 4 5 6 7 8
G
mCherry-G45
R375A
Flag-UBC9-WT - + - +
Flag-UBC9-DN + - + -
Myc-SUMO3 + + + +
Blot: mCherry
- 250 kDa
- 150 kDa
- 100 kDa
- 75 kDa
- 50 kDa
Blot: FLAG
- 20 kDa
Blot: β actin
- 37 kDa
Blot: Myc
- 250 kDa
- 150 kDa
- 100 kDa
- 75 kDa
- 50 kDa
- 37 kDa
- 25 kDa
- 20 kDa
- 15 kDa
1 2 3 4

Figure 4

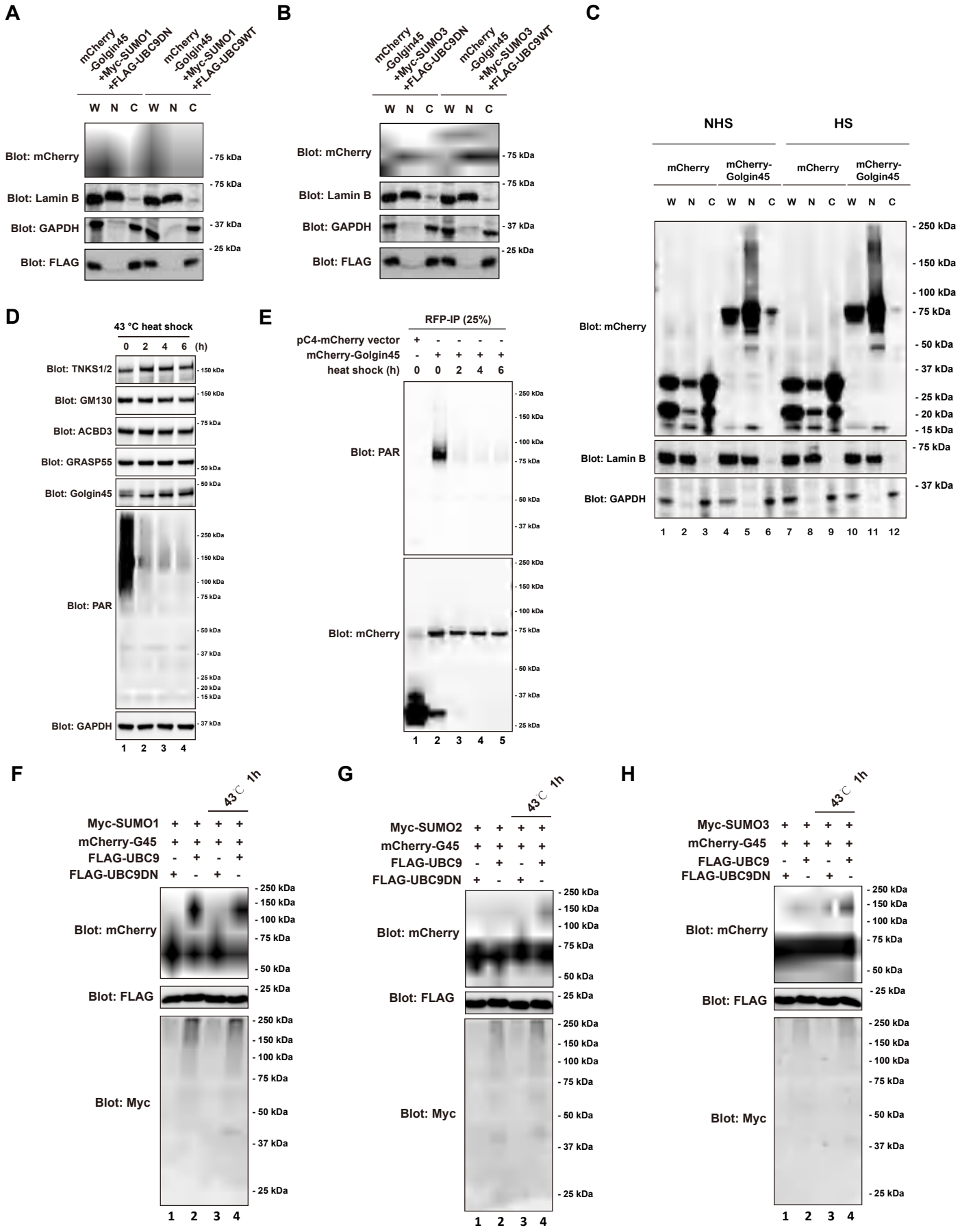
A
mCherry -Golgin45 +Myc-SUMO1 +FLAG-UBC9DN
mCherry -Golgin45 +Myc-SUMO1 +FLAG-UBC9WT
W N C W N C
Blot: mCherry
Blot: Lamin B
Blot: GAPDH
Blot: FLAG
- 75 kDa
- 75 kDa
- 37 kDa
- 25 kDa
B
mCherry -Golgin45 +Myc-SUMO3 +FLAG-UBC9DN
mCherry -Golgin45 +Myc-SUMO3 +FLAG-UBC9WT
W N C W N C
Blot: mCherry
Blot: Lamin B
Blot: GAPDH
Blot: FLAG
- 75 kDa
- 75 kDa
- 37 kDa
- 25 kDa
C
NHS
HS
mCherry
mCherry-Golgin45
mCherry
mCherry-Golgin45
W N C W N C W N C W N C
Blot: mCherry
Blot: Lamin B
Blot: GAPDH
- 250 kDa
- 150 kDa
- 100 kDa
- 75 kDa
- 50 kDa
- 37 kDa
- 25 kDa
- 20 kDa
- 15 kDa
- 75 kDa
- 37 kDa
1 2 3 4 5 6 7 8 9 10 11 12
D
43 °C heat shock
0 2 4 6 (h)
Blot: TNKS1/2
Blot: GM130
Blot: ACBD3
Blot: GRASP55
Blot: Golgin45
Blot: PAR
Blot: GAPDH
- 150 kDa
- 150 kDa
- 75 kDa
- 50 kDa
- 50 kDa
- 250 kDa
- 150 kDa
- 100 kDa
- 75 kDa
- 50 kDa
- 37 kDa
- 25 kDa
- 20 kDa
- 15 kDa
- 37 kDa
1 2 3 4
E
RFP-IP (25%)
pC4-mCherry vector + - - - -
mCherry-Golgin45 - + + + +
heat shock (h) 0 0 2 4 6
Blot: PAR
Blot: mCherry
- 250 kDa
- 150 kDa
- 100 kDa
- 75 kDa
- 50 kDa
- 37 kDa
- 25 kDa
1 2 3 4 5
F
43℃ 1h
Myc-SUMO1 + + + +
mCherry-G45 + + + +
FLAG-UBC9 - + - +
FLAG-UBC9DN + - + -
Blot: mCherry
Blot: FLAG
Blot: Myc
- 250 kDa
- 150 kDa
- 100 kDa
- 75 kDa
- 50 kDa
- 25 kDa
- 37 kDa
1 2 3 4
G
43℃ 1h
Myc-SUMO2 + + + +
mCherry-G45 + + + +
FLAG-UBC9 - + - +
FLAG-UBC9DN + - + -
Blot: mCherry
Blot: FLAG
Blot: Myc
- 250 kDa
- 150 kDa
- 100 kDa
- 75 kDa
- 50 kDa
- 25 kDa
- 37 kDa
1 2 3 4
H
43℃ 1h
Myc-SUMO3 + + + +
mCherry-G45 + + + +
FLAG-UBC9 - + - +
FLAG-UBC9DN + - + -
Blot: mCherry
Blot: FLAG
Blot: Myc
- 250 kDa
- 150 kDa
- 100 kDa
- 75 kDa
- 50 kDa
- 25 kDa
- 37 kDa
1 2 3 4

Figure 5

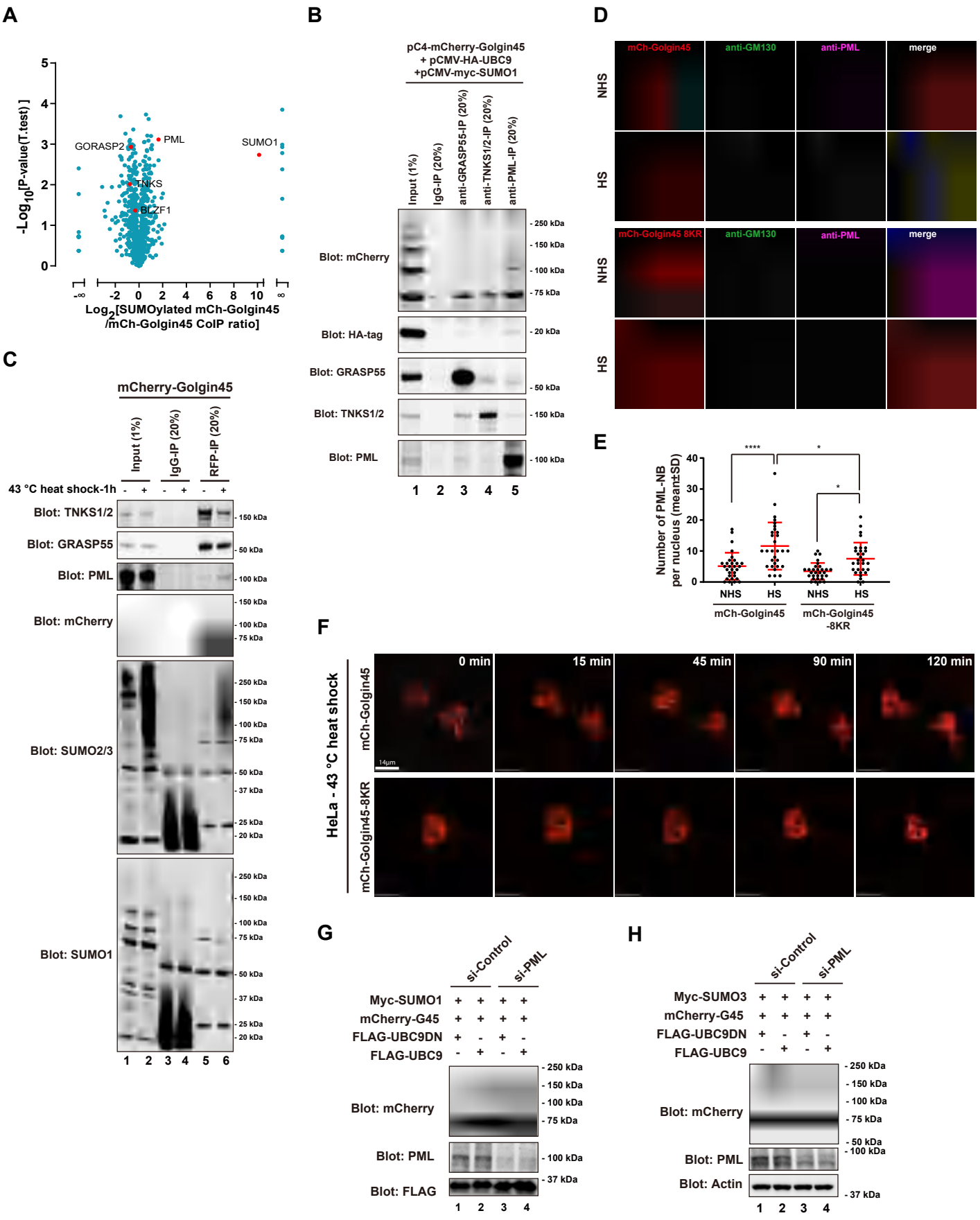
A
-Log10[P-value(T.test)]
GORASP2
PML
SUMO1
TNKS
BCZF1
Log2[SUMOylated mCh-Golgin45 /mCh-Golgin45 CoIP ratio]
B
pC4-mCherry-Golgin45 + pCMV-HA-UBC9 +pCMV-myc-SUMO1
Input (1%)
IgG-IP (20%)
anti-GRASP55-IP (20%)
anti-TNKS1/2-IP (20%)
anti-PML-IP (20%)
Blot: mCherry
Blot: HA-tag
Blot: GRASP55
Blot: TNKS1/2
Blot: PML
C
mCherry-Golgin45
43 °C heat shock-1h
Blot: TNKS1/2
Blot: GRASP55
Blot: PML
Blot: mCherry
Blot: SUMO2/3
Blot: SUMO1
D
mCh-Golgin45
anti-GM130
anti-PML
merge
NHS
HS
mCh-Golgin45 8KR
E
Number of PML-NB per nucleus (mean±SD)
NHS
HS
mCh-Golgin45
mCh-Golgin45 -8KR
F
HeLa - 43 °C heat shock
mCh-Golgin45
mCh-Golgin45-8KR
0 min
15 min
45 min
90 min
120 min
G
si-Control
si-PML
Myc-SUMO1
mCherry-G45
FLAG-UBC9DN
FLAG-UBC9
Blot: mCherry
Blot: PML
Blot: FLAG
H
Myc-SUMO3
Blot: Actin

Figure 6

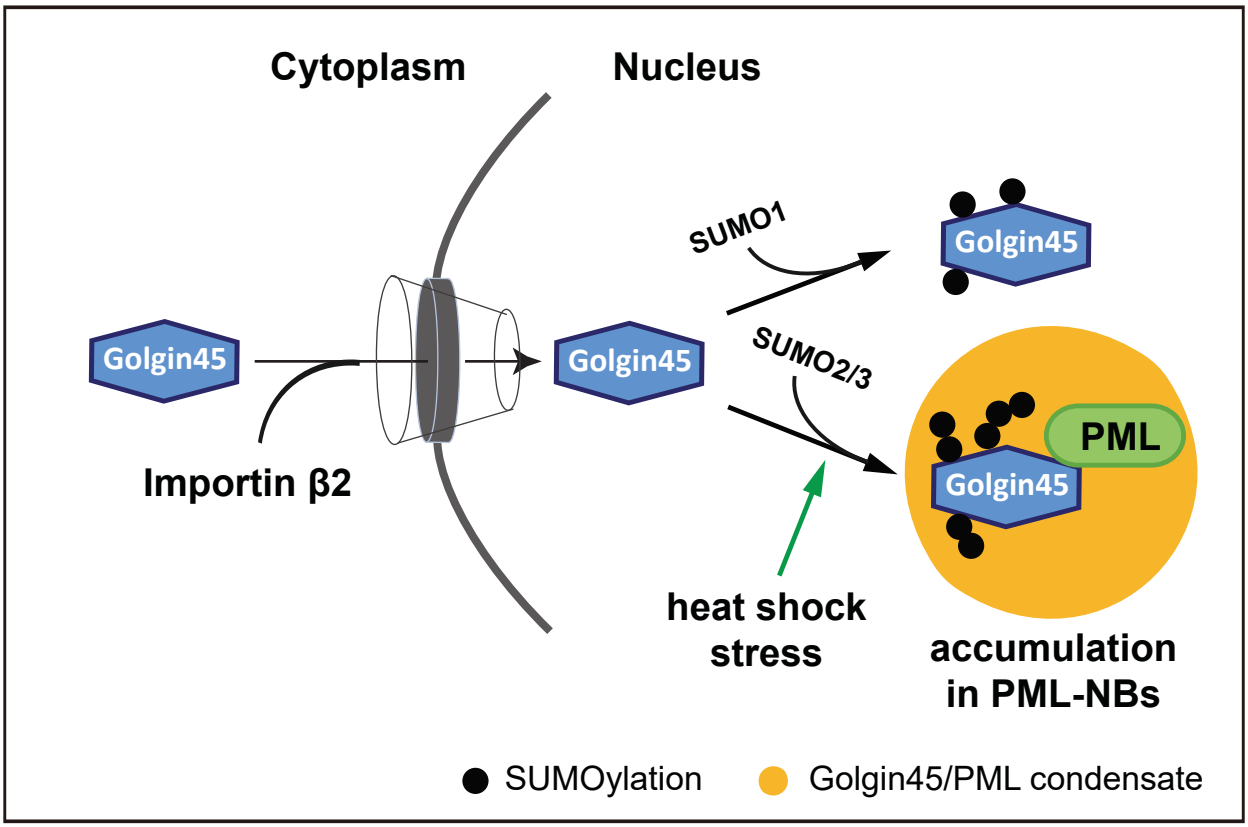
Cytoplasm
Nucleus
Golgin45
Importin β2
Golgin45
SUMO1
SUMO2/3
Golgin45
PML
Golgin45
heat shock stress
accumulation in PML-NBs
SUMOylation
Golgin45/PML condensate

Supplementary Figure 1

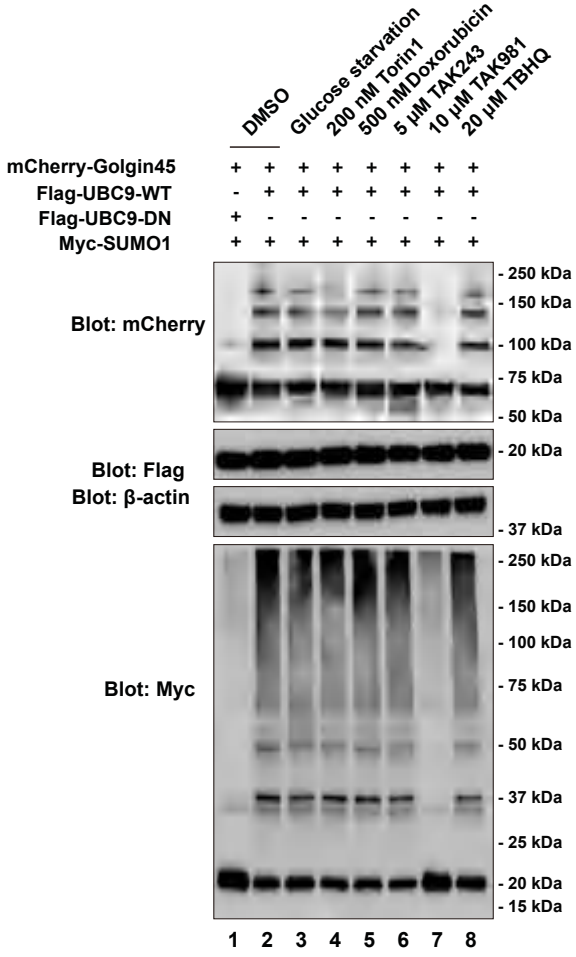

Supplementary Figure 2

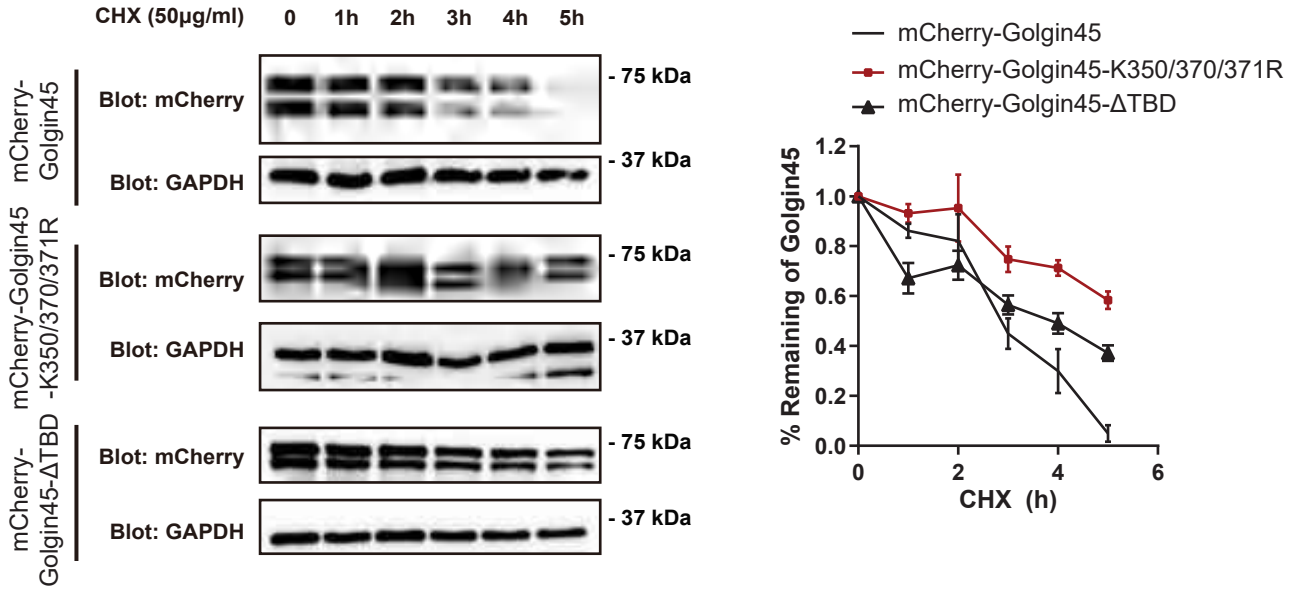

Supplementary Figure 3
Unprocessed images of all blots

Unprocessed western blots in main figures. Some blots were cut into several pieces and incubated with different antibodies.

Unprocessed blots of Figure 1

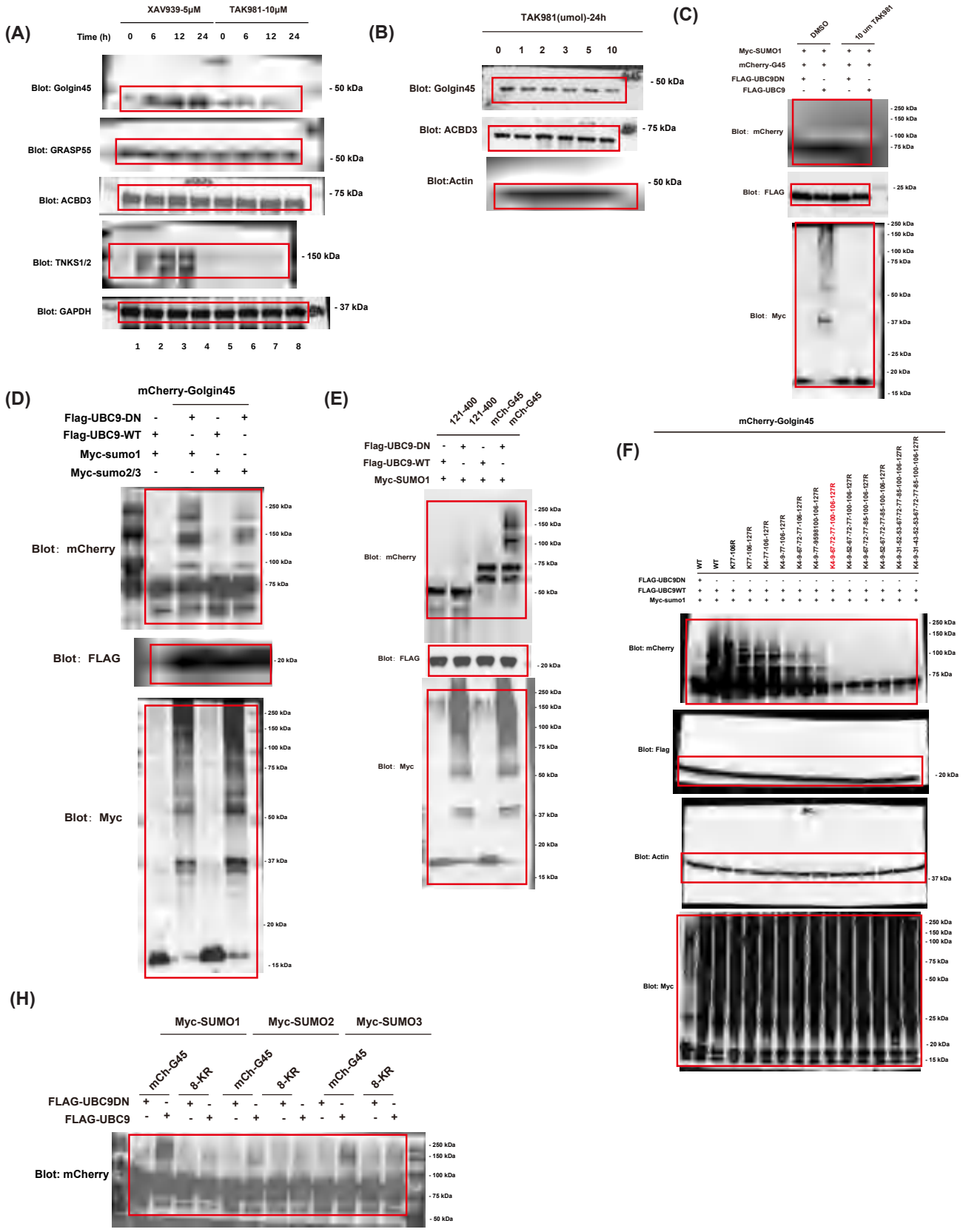

Unprocessed blots of Figure 1

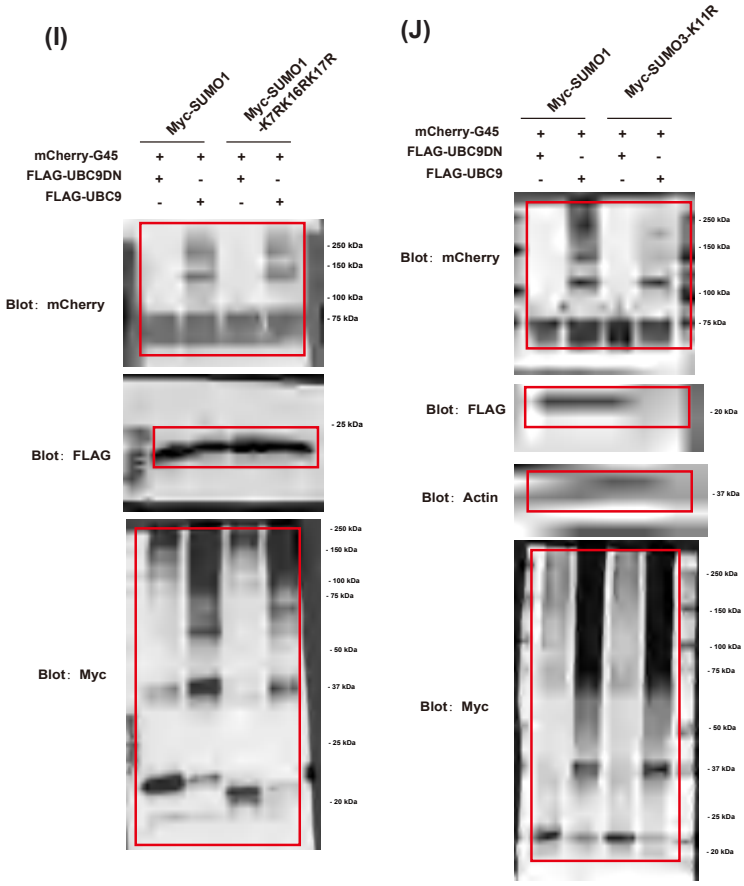

Unprocessed blots of Figure 2

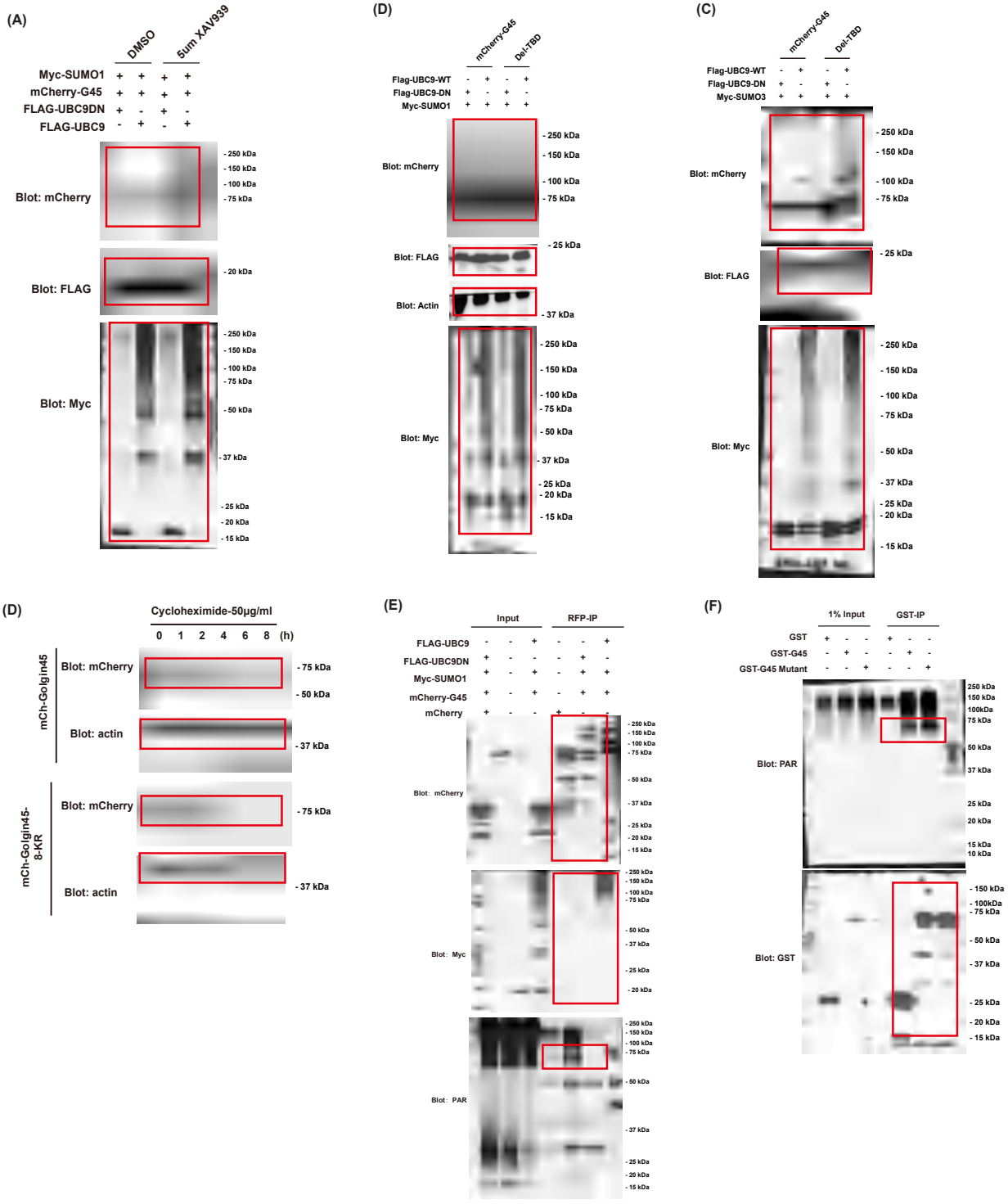

Unprocessed blots of Figure 3

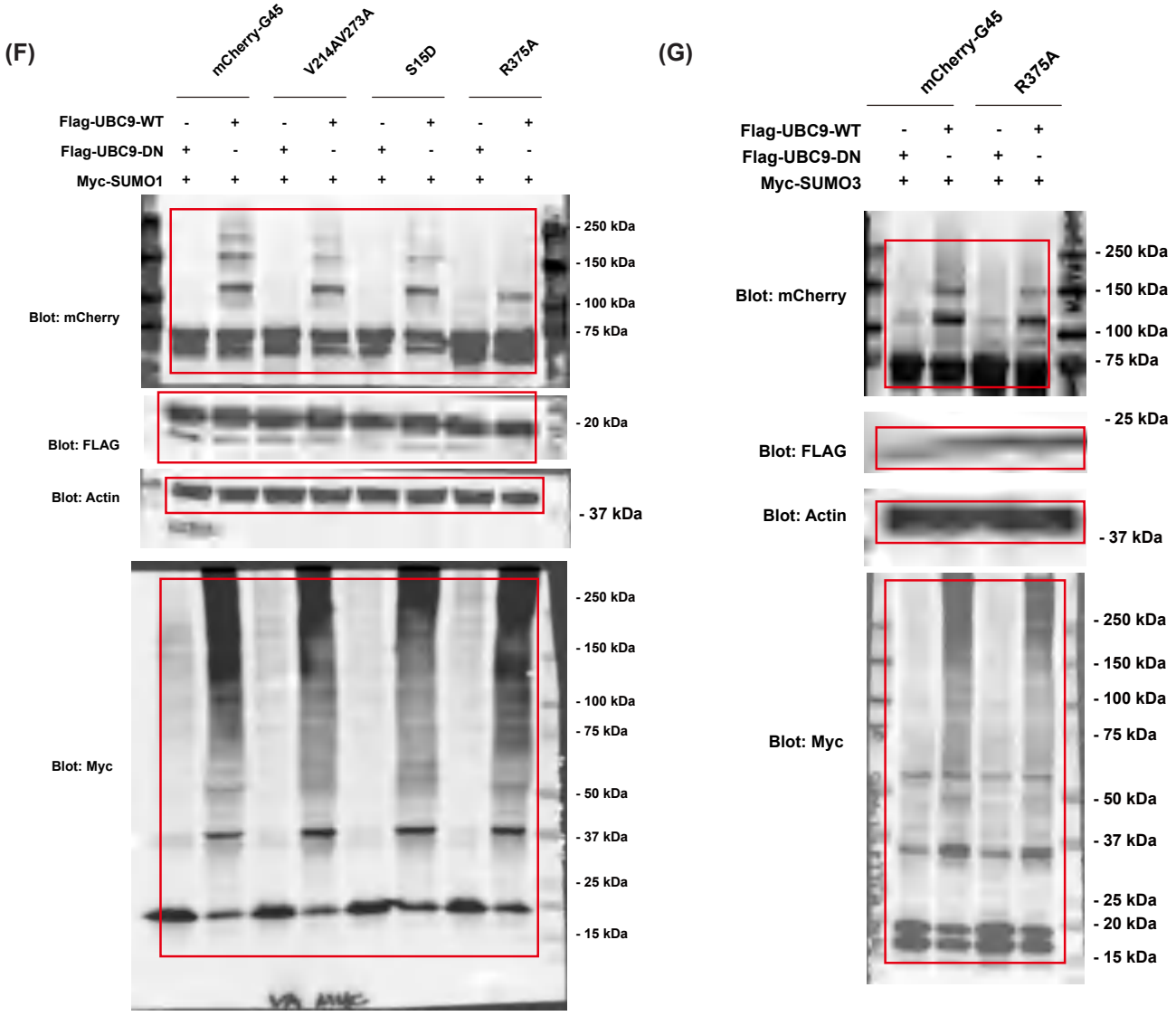

Unprocessed blots of Figure 4

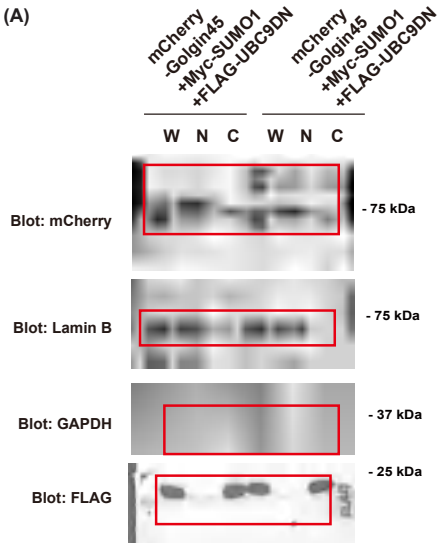

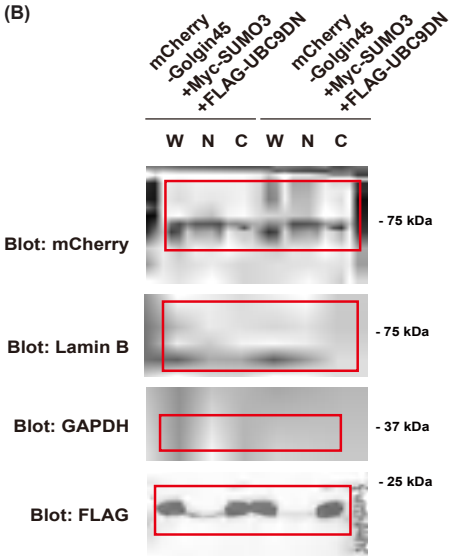

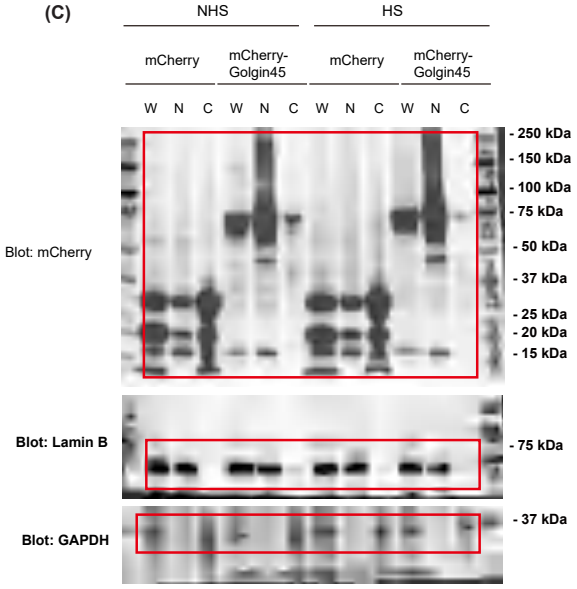

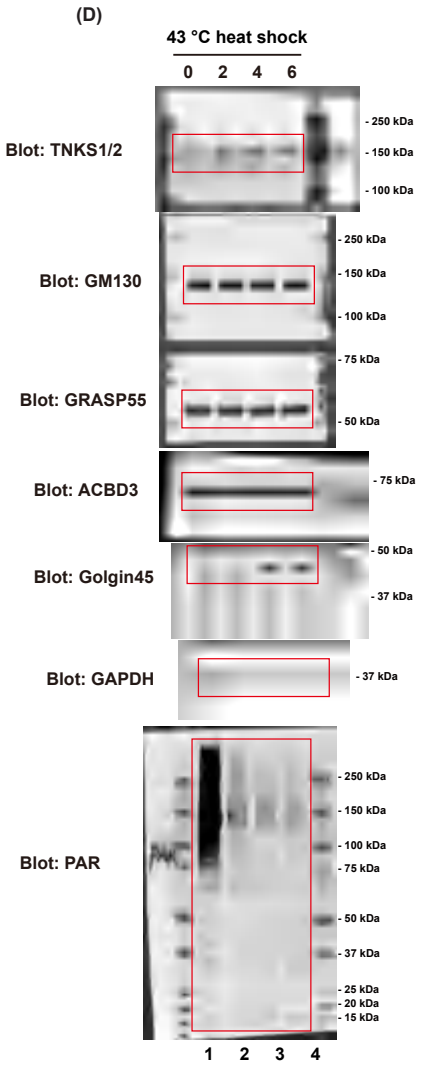

Unprocessed blots of Figure 4

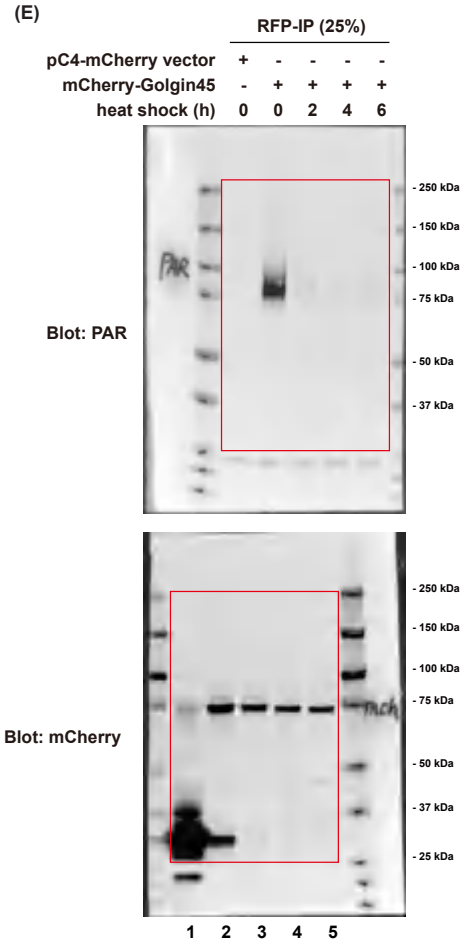

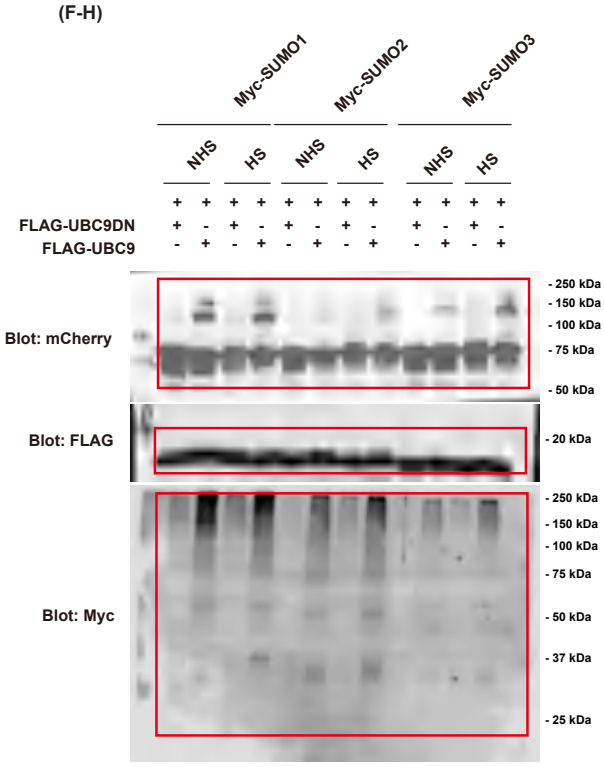

Unprocessed blots of Figure 5

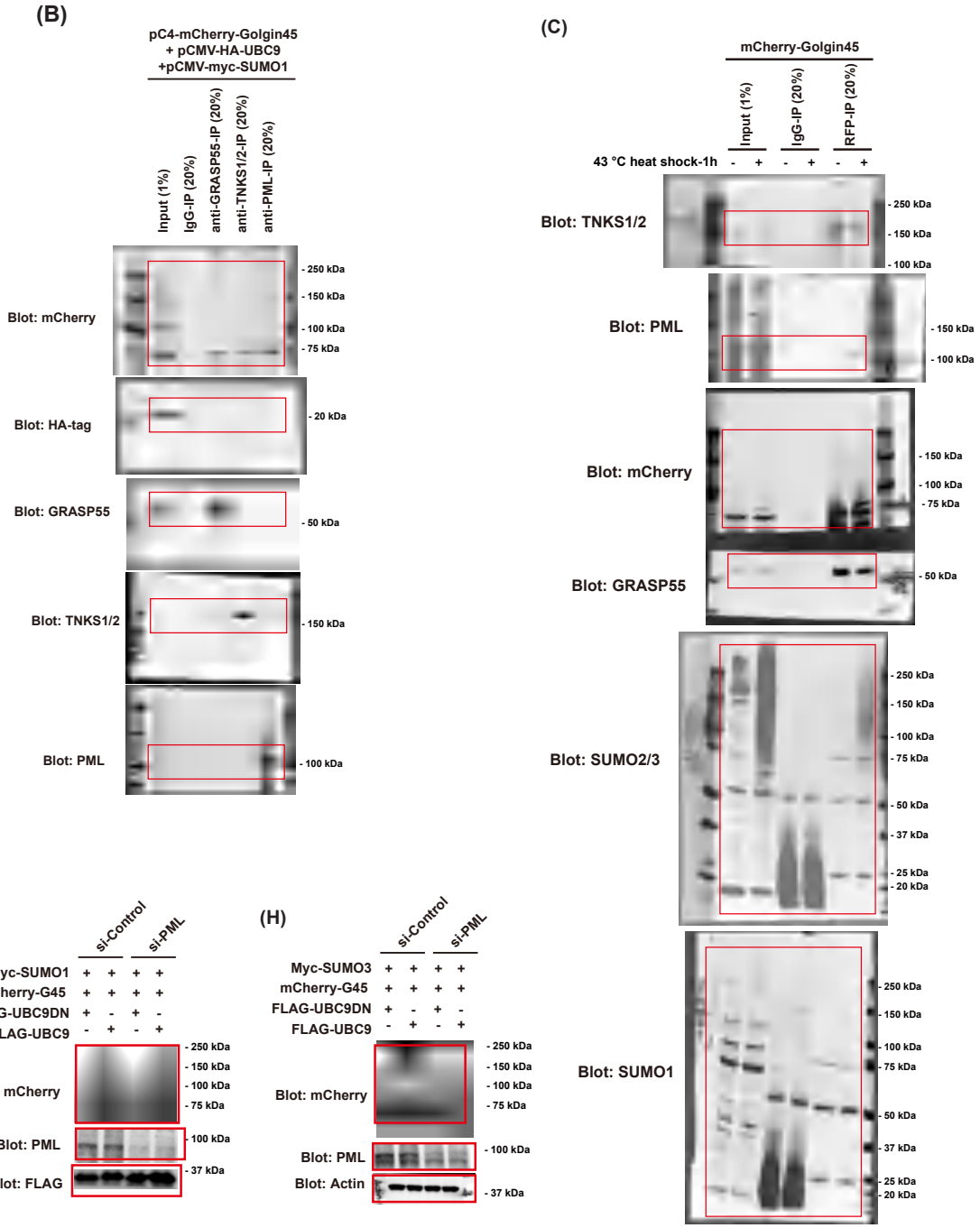

(Supplementary Figure 1)

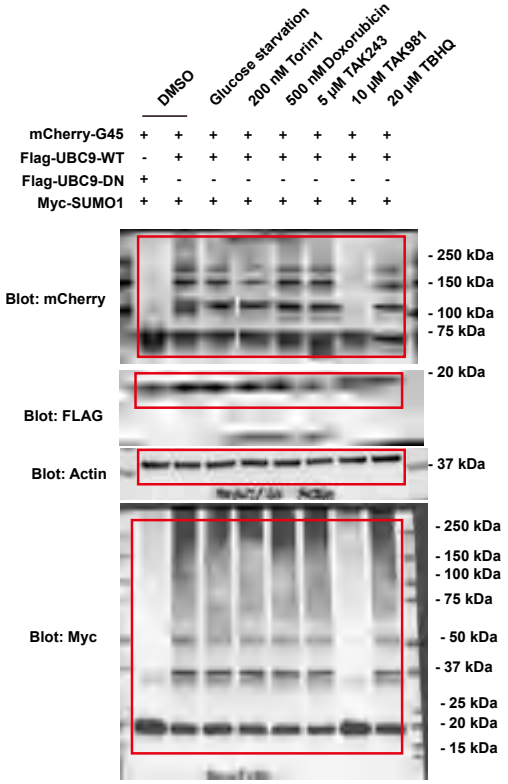

(Supplementary Figure 2)

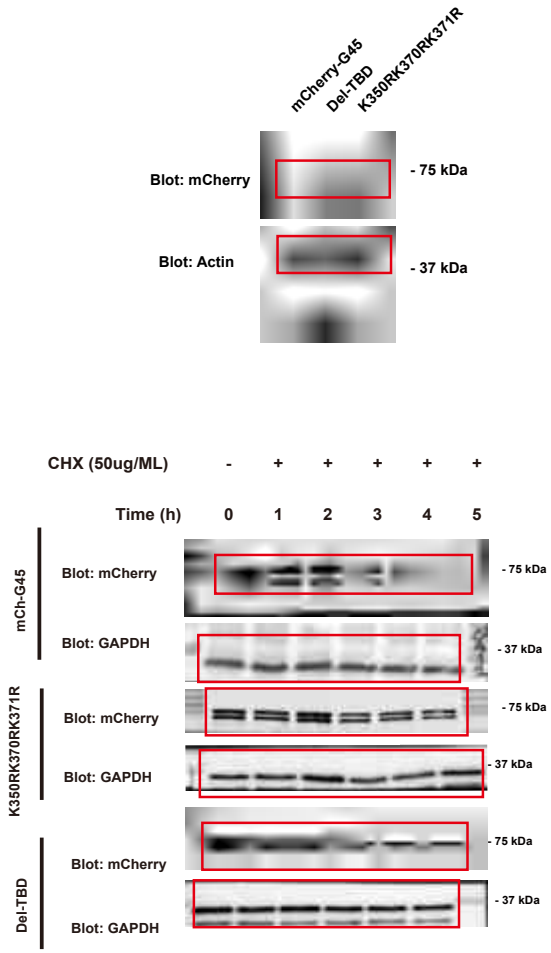

Supplementary Files

This is a list of supplementary files associated with this preprint. Click to download.

- supplementaryFigure1.tif
- supplementaryFigure2.tif